

Forest-Chat: Adapting Vision-Language Agents for Interactive Forest Change Analysis

James Brock^{a,*}, Ce Zhang^b, Nantheera Anantrasirichai^a

^aSchool of Computer Science, University of Bristol, Merchant Venturers Building, 75 Woodland Road, Bristol, BS8 1UB, Bristol, United Kingdom

^bSchool of Geographical Sciences, University of Bristol, University Road, Bristol, BS8 1SS, Bristol, United Kingdom

Abstract

The increasing availability of high-resolution satellite imagery, together with advances in deep learning, creates new opportunities for enhancing forest monitoring workflows. Two central challenges in this domain are pixel-level change detection and semantic change interpretation, particularly for complex forest dynamics. While large language models (LLMs) are increasingly adopted for data exploration, their integration with vision-language models (VLMs) for remote sensing image change interpretation (RSICI) remains underexplored, especially beyond urban environments. This paper introduces Forest-Chat, an LLM-driven agent designed for integrated forest change analysis. The proposed framework enables natural language querying and supports multiple RSICI tasks, including change detection, change captioning, object counting, deforestation percentage estimation, and change reasoning. Forest-Chat builds upon a multi-level change interpretation (MCI) vision-language backbone with LLM-based orchestration, and incorporates zero-shot change detection via AnyChange together with an interactive point-prompt interface to support fine-grained user guidance. To facilitate adaptation and evaluation in forest environments, we introduce the Forest-Change dataset, comprising bi-temporal satellite imagery, pixel-level change masks, and multi-granularity semantic change captions generated through a combination of human annotation and rule-based methods. Experimental results show that Forest-Chat achieves mIoU and BLEU-4 scores of 67.10% and 40.17% on the Forest-Change dataset, and 88.13% and 34.41% on LEVIR-MCI-Trees, a tree-focused subset of LEVIR-MCI for joint change detection and captioning. In contrast, when Forest-Chat is used in a zero-shot capacity for change detection, it achieves mIoU scores of 59.51% and 47.32% on the two datasets respectively. These findings highlight the potential of interactive, LLM-driven RSICI systems to improve accessibility, interpretability, and analytical efficiency for forest change analysis. Two new datasets and code are publicly available at <https://github.com/JamesBrockUoB/ForestChat>.

Keywords: Vision-Language models, Multi-task learning, Change interpretation, Zero-shot change detection, LLM agents

1. Introduction

Of the world's terrestrial landmass, forests account for 31 percent of the total area, with tropical forests accounting for nearly half of this total (Canton, 2021). Forests provide habitat for up to 80% of land-based species and represented a total carbon stock of 662 gigatonnes in 2020 (Canton, 2021; Lines et al., 2022). For a multitude of species, forests provide an abundance of resources, both in terms of physical materials and wider ecosystem services such as water and nutrient recycling and climate regulation via carbon sequestration (Lines et al., 2022; Ouaknine et al., 2025; Wegler and Kuenzer, 2024). These factors contribute to the central role of forests in adapting to and mitigating climate change. However, anthropogenic pressures and the accelerating frequency of extreme weather events are detrimentally impacting both the health and integrity of global forest ecosystems (Wegler and Kuenzer, 2024). Global forest cover is in a constant state of flux due to a myriad of pressures, such as industrial logging, agricultural expansion, wildfires, extreme weather events, disease, and pests (Hansen et al., 2013).

Monitoring and quantifying the types, extent, and locations of

changes across vast regions is crucial for mapping and understanding forest dynamics for both policymakers and researchers (Wegler and Kuenzer, 2024). Effective monitoring of forest loss, degradation, and recovery increasingly relies on automated data collection and processing pipelines as traditional field-surveys become insufficient to meet demand (Ouaknine et al., 2025). The last decade has seen researchers become inundated with remote sensing (RS) imagery capable of providing sub-metre pixel resolution across expansive areas (Lines et al., 2022). The rich image history, spatial and temporal density, and range of freely available sensor modalities enables a better understanding of forest ecosystems as more efficient and low-cost monitoring technologies are developed and adopted (Wegler and Kuenzer, 2024; Isaienkova et al., 2020; Lines et al., 2022).

As access to forest-specific datasets and benchmarks have increased, spurred on by tools such as Google Earth Engine (GEE) (Gorelick et al., 2017), a corresponding rise in deep learning (DL) and other artificial intelligence (AI) methods for forest analysis has been observed (Yun et al., 2024; Isaienkova et al., 2020). A review by Yun et al. (2024) highlights a growing publication trend in the field across multiple tasks, including but not limited to: forest resource assessment (Nguyen et al., 2024), forest ecological disturbance monitoring (Lee et al., 2023), for-

*Corresponding author. Email address: james.brock@bristol.ac.uk

est parameter retrieval at individual scale (Lin et al., 2024), and tree organ-level measurement (Cai et al., 2023). A historical reliance on CNN-based architectures for the majority of data modalities and prediction tasks (e.g. classification, segmentation, object detection, and regression) has recently given way to Transformers (Vaswani et al., 2017), attention-based architectures, and hybrid architectures. Hewarathna et al. (2024) exemplify this paradigm shift by proposing a Siamese Attention U-Net model for forest ecosystem change detection.

The recent research trend of exploring large language models (LLMs) as assistants to human domain experts (Ge et al., 2023) has propagated out to the task of remote sensing image change interpretation (RSICI) (Li et al., 2024a; Liu et al., 2024). Specifically, Vision-Language Models (VLMs) have been applied to RS tasks to address longstanding methodological shortcomings in AI, particularly DL-based methods (Li et al., 2024c). Gaining an enhanced semantic understanding of objects and their relationships both spatially and temporally in RS scenes has largely been neglected by vision-only models (Li et al., 2024a,c). By harnessing multiple modalities and semantic reasoning capabilities, VLMs are able to establish connections between visual concepts, subsequently demonstrating improved performance, especially on out-of-distribution data (Li et al., 2024c; Mu et al., 2025). The culmination of these systems has resulted in the proposal of chatbots capable of assisting human users in RS image processing, with the capability of providing zero-shot/open-vocabulary visual understanding (Li et al., 2024c; Irvin et al., 2025; Liu et al., 2024; Du et al., 2023).

Several prescient review papers have highlighted the opportunities and challenges for large foundation model-assisted remote sensing change detection (RSCD) and remote sensing image change captioning (RSICC) for augmenting the capabilities of RS domain experts (Zhang and Wang, 2024; Zou et al., 2025; Peng et al., 2025; Li et al., 2024a,b). Promising research directions include leveraging the powerful zero-shot performance of VLMs for RSCD and RSICC tasks (Peng et al., 2025; Li et al., 2024b), incorporating multi-modal data streams into AI training (Li et al., 2024a), and deeper explorations of interactive human-machine collaboration (Peng et al., 2025; Li et al., 2024a). Developing conversational agents with access to RSICI-specific tooling capable of providing interactive and comprehensive change interpretation and analysis represents a significant advancement (Liu et al., 2024; Irvin et al., 2025). Liu et al. (2022) provide valuable insights into the rapid emergence of this field by categorising the development of new spatio-temporal VLMs for RS tasks (RS-STVLMs). Models capable of dual change detection and captioning (CDC) that incorporate LLM agents capable of task orchestration and exploratory conversations are of particular interest here. The work of Change-Agent (Liu et al., 2024) specifically represents a paradigm shift in RS-STVLM development - being the first VLM capable of dual CDC to be embedded within an agent for spatio-temporal RS tasks.

While frameworks like Change-Agent demonstrate the poten-

tial of natural language interfaces for RS tasks, they often require large task-specific training datasets to align change detection outputs with semantic descriptions (e.g. TEOChat (Irvin et al., 2025)). In parallel, recent studies have questioned whether current vision–language foundation models can reliably support zero-shot change interpretation. For single-image captioning, recent works (Zhang and Wang, 2024; Zeng et al., 2024) have documented the tendency for these models to hallucinate, fail to align generated text with the image context, or produce incomplete sentences. To date, no frameworks have been proposed for purpose-built zero-shot image change captioning. Benchmarking studies have shown that generalised foundational VLMs like GPT-4V (openai et al., 2023) perform poorly on zero-shot change captioning tasks (Zhang and Wang, 2024). Descriptions are often vague, inconsistent, or fail to capture subtle or quantitative aspects of change inherent to the scene. Due to GPT-4V’s training data being predominantly based on natural images, the model’s efficacy for Earth observation tasks is limited due to weak spatial reasoning capabilities (Zhang and Wang, 2024), especially for fine-grained, quantitative-based tasks (e.g. object change counting). In contrast, recent work has demonstrated stronger potential for pixel-level change detection. Specifically, "Segment Any Change" by Zheng et al. (2024) introduces a promptable, zero-shot semantic change detection segmentation model called AnyChange. Their work extends the foundational Segment Anything Model (SAM) (Kirillov et al., 2023) by employing a novel training-free method called bi-temporal latent matching to extract semantic similarities between two RS images. Although such methods offer training-free zero-shot capabilities, effective domain-specific change interpretation - particularly in forest applications - remains challenging due to subtle structural variations, seasonal phenology, and heterogeneous disturbance patterns, and thus still greatly benefits from purpose-built architectures and tailored datasets.

To address these challenges, this work introduces Forest-Chat (Fig. 1), a Change-Agent inspired VLM-agent system adapted to interactive forest change analysis. The Multi-level Change Interpretation (MCI) model is retained as the ‘eyes’ of the system, capable of dual CDC, whilst an LLM is employed as the ‘brain’. AnyChange is additionally incorporated into the framework to enable zero-shot and interactive point-query based change segmentation as an alternative to computationally intensive training. Finally, the system is augmented with forest-change-specific capabilities to enhance user understanding. To support the development of this system, this paper introduces the Forest-Change dataset. It is the first dataset capable of providing both pixel-level bi-temporal change masks and semantic-level change captions solely aimed at forest change analysis. The Forest-Chat agent is capable of providing a convenient and conversational interface for researchers to interactively explore forest change events whilst reducing cognitive load and manual analysis workloads. More broadly, this paradigm further opens opportunities for expert-in-the-loop analysis, allowing knowledge-driven reasoning and shared expertise to be integrated into the understanding of long-term and

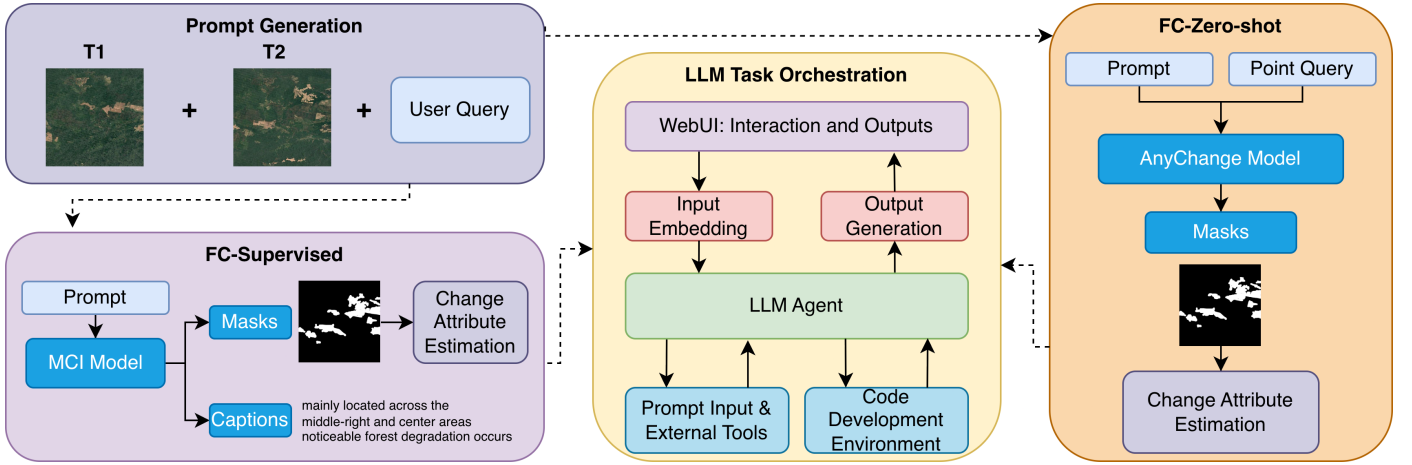


Figure 1: Overview of the Forest-Chat system. Forest-Chat is supplied with the MCI (Liu et al., 2024) and AnyChange (Zheng et al., 2024) models (respectively designated as FC-Supervised and FC-Zero-shot when integrated into the Forest-Chat system) to operate as its eyes, and an LLM as the brain. The proposed Forest-Change and LEVIR-MCI-Trees datasets are used as a data foundation for training and adapting the MCI model for forest change analysis.

heterogeneous forest dynamics. Extensive experiments benchmark Forest-Chat’s supervised and zero-shot change interpretation capabilities against contemporary models on the introduced Forest-Change dataset and a LEVIR-MCI (Liu et al., 2024) dataset subset. Further ablation studies are conducted to investigate the influence of backbone model size and various multi-task learning optimisation approaches on model performance.

The contributions of this work are outlined below.

- **Forest-Chat** is presented as an interactive forest change analysis tool that incorporates the MCI model (FC-Supervised) for pixel-level change detection and captioning (CDC), and the zero-shot AnyChange model (FC-Zero-shot) solely for pixel-level change detection. Additional tooling that further analyses the outputs of these models is provided to enable deeper forest change understanding. The LLM-driven orchestration and dialogue enables a flexible and innovative approach for exploring RS imagery. Forest-Chat can perform various tasks relating to temporal forest analysis. Extensive experiments on two disparate datasets explores several architectural components of the MCI model.
- **Forest-Change** is proposed as a demonstration dataset for RSICI in forest applications by incorporating bi-temporal image pairs, corresponding change masks and supplementary captions that describe the degree, location, and patterns of observed deforestation.
- **LEVIR-MCI-Trees** is additionally included as a benchmarking dataset to contrast against Forest-Change. It is a subset of LEVIR-MCI that only contains examples with captions containing tree cover changes. This larger, urban-focused dataset enables an analysis of generalisation capabilities against the smaller, scene restricted Forest-Change dataset.
- **Interactive point querying** for the AnyChange model

is made available inside the Forest-Chat interface. This extension aims to improve the user experience when utilising Forest-Chat for zero-shot change detection.

- An **image change captioning interface** is introduced to assist with generating captions for bi-temporal image CDC datasets. Users are able to manually and automatically generate captions that can provide varied and informative descriptions pertaining to the visible changes within the RS imagery.

2. Related Work

This work concentrates on vision-language agents (VLAs) capable of multi-task learning for remote sensing image change interpretation (RSICI) tasks. Research directions into RS-VLAs are increasing in both maturity and diversity, but the areas relevant to this work include RSICI, multi-task learning (MTL), foundation and vision-language models (VLMs), and large language model (LLMs) agents.

2.1. Remote Sensing Image Change Interpretation (RSICI)

RSICI as it currently stands encompasses the tasks of RS change detection and captioning (CDC), capable of being applied across a diverse range of remote sensing data modalities and resolutions (Liu et al., 2024). RSCD is a fundamental spatio-temporal task aimed at identifying changes between multi-temporal images of a given area; either as binary predictions, or across multiple categories for deeper semantic understanding and causal attribution (Liu et al., 2025; Li et al., 2025). DL RSCD research has primarily revolved around RNN- and CNN-based models, which automatically learn hierarchical and multi-temporal features, but are constrained by local temporal and spatial receptive fields respectively. Transformers overcame this limitation by incorporating self-attention mechanisms, enabling the capture of global context and long-range dependencies that are crucial for interpreting complex scenes

(Shi et al., 2024). Recently, state-space models (e.g. Mamba (Gu and Dao, 2024)) have emerged, with adaptations made for RSCD (Chen et al., 2024; Zhang et al., 2025a), which offer a promising alternative for efficient long-dependency modelling that doesn't incur the quadratic complexity of transformers (Liu et al., 2025). Progress has been further accelerated by the widespread adoption of multi-scale feature fusion techniques, Siamese networks, and pretrained backbone networks for extracting high-level semantic features from multi-temporal RS imagery (Shi et al., 2024). Zero-shot RSCD was recently achieved by the *AnyChange* model (Zheng et al., 2024) which leverages the Segment Anything Model (SAM) (Kirillov et al., 2023) to provide annotation-free change analysis without task-specific fine-tuning.

RSCD is fundamentally limited to explaining "what" has changed, as compared to the deeper questions of "why" and "how". The next task is to provide semantic change descriptions that bridge the gap between computer vision (CV) and natural language processing (NLP) (Shi et al., 2024). RSICC - being a combination of image captioning and change detection - demands precise visual change recognition and robust language generation capabilities to ensure the creation of correct and natural language (Liu et al., 2025; Tao et al., 2025). Contemporary methods often adopt a three-stage architecture pipeline, typically incorporating advanced CNNs, transformers, and Vision Transformers (ViTs), to extract robust semantic change representations and produce coherent textual descriptions. This three-stage paradigm was effectively established and popularised by RSICCformer (Liu et al., 2022), which coupled a CNN-based visual feature extractor with a dual-branch Siamese transformer encoder to enhance change discrimination, and a transformer caption decoder to generate coherent descriptions. The LEVIR-CC (Liu et al., 2022) benchmark dataset accompanying RSICCformer has since spurred the development of related architectures. CD4C (Li et al., 2025) integrates a supervised change-detection branch and a two-stream fusion module to adaptively handle samples with reliable or unreliable change cues. KCFI (Yang et al., 2025a) employs ViT encoders, a key-change feature perceiver, and an instruction-tuned LLM decoder jointly trained with pixel-level change detection to improve semantic grounding. This work culminates in the MCI model (Liu et al., 2024), the first model to fully unify RSCD and RSICC in a single multi-task learning framework, simultaneously generating change masks and textual descriptions, and supported by the LEVIR-MCI dataset for joint evaluation.

2.2. Multi-Task Learning (MTL)

MTL has recently been explored as a means of jointly modelling RSCD and RSICC, leveraging the complementary relationship being spatial change cues and semantic descriptions (Shi et al., 2024). Representations learned for RSCD improve localisation in captioning, while RSICC provides high-level semantic guidance that strengthens change delineation, all while reducing overall training and optimisation costs (Shi et al., 2024).

In a unified framework for RSCD and RSICC, MTL can be formalised as the joint learning of pixel-level change masks and semantic descriptions: $(M, S) = f_{CD,CC}(I)$ where $I = \{I_1, I_2, \dots, I_m\}$ represents a temporal sequence of RS images, M is a pixel-level change mask that offers granular, pixel-accurate localisation of changes, and S is a high-level semantic narrative of those changes (Liu et al., 2025; Zhang and Yang, 2021).

A central challenge to MTL frameworks is ensuring that no single task dominates optimisation, since RSCD and RSICC benefit from - but also compete for - shared representations (Shi et al., 2024; Crawshaw, 2020). Existing work addresses this through architectural design choices and parameter-sharing strategies. Hard parameter sharing uses common encoders with task-specific heads, reducing overfitting risk and parameter counts. Conversely, soft parameter sharing maintains separate task-specific modules whose parameters are regularised through joint loss functions to enforce similarity, capturing shared features but increasing computational burden (Shi et al., 2024; Crawshaw, 2020).

Optimising task loss balancing is another relevant MTL research direction, with approaches evolving from inflexible manual weight assignments towards dynamic weighting strategies that adjust task contributions during training, including uncertainty-based weighting (Kendall et al., 2018) and GradNorm (Chen et al., 2018). Subsequent work tackles gradient interference explicitly by treating MTL as a multi-objective task (Sener and Koltun, 2018), or by adjusting gradient directions to promote cooperative updates (Yu et al., 2020)

2.3. Vision-Language Models (VLMs)

Vision-language models (VLMs) have seen rapid progress alongside recent advances in LLMs such as GPT (openai et al., 2023) and LLaMA (Touvron et al., 2023), combining instruction-following with visual feature analysis. VLMs typically pair a pretrained visual encoder — such as the contrastively trained CLIP model (Radford et al., 2021), or ViTs — with an LLM through a projection or transformation module that maps visual embeddings into the language model's input space (Li et al., 2024d; Tao et al., 2025). This alignment allows LLMs to link user instructions to extract visual information, providing support for generalised tasks such as visual-question-answering, captioning, and zero-shot transfer learning (Lu et al., 2025; Li et al., 2024b). These capabilities have made VLMs an increasingly common choice for RS applications, particularly through large foundation models pretrained on massive and diverse datasets using task-agnostic objectives (Li et al., 2024c; Zhang et al., 2025b; Liu et al., 2024; Irvin et al., 2025; Liu and Lian, 2024; Li et al., 2024d; Hu et al., 2025; Zhang et al., 2024b). RS applications benefit from domain-specific pretraining across varying sensors, resolutions, and imaging geometries, while self-supervised and zero-shot learning helps reduce the reliance on exhaustive annotation (Peng et al., 2025; Lu et al., 2025). Text prompting and question-and-answer interactions further support context-aware interpretation, helping models link ambiguous visual patterns to high-

level semantic concepts (e.g. deforestation) (Peng et al., 2025; Li et al., 2024a).

Despite strong performance on natural imagery, general-purpose multimodal LLMs such as GPT-4V and LLaVa (openai et al., 2023; Bazi et al., 2024) perform poorly on RS and change-related tasks due to domain mismatch Zhang and Wang (2024). One response has been to adapt LLM-driven, task-specific spatio-temporal VLMs to RS vision-language understanding tasks (Liu et al., 2025). Examples include KCFI (Yang et al., 2025a) and Semantic-CC (Zhu et al., 2024), which fine-tune visual modules or lightweight LLM components for change-focused tasks. Semantic-CC additionally integrates SAM-derived change masks (Kirillov et al., 2023). Related efforts such as Change-UP (Yang et al., 2025b) and ChangeMinds (Wang et al., 2024) target joint RSCDC within unified architectures, end-to-end architectures. Change-UP emphasises multi-scale change-aware feature fusion and semantic query alignment to enhance differential representations. ChangeMinds, by contrast, introduces a change-aware LSTM and a cross-attention predictor to learn shared spatiotemporal features for both change detection and captioning. However, these approaches - whether task-specific or unified - remain narrow in objective scope, relying on specialised labelled datasets that limit generalisation (e.g. RSGPT (Hu et al., 2025)) (Liu et al., 2025). Another direction aims to unify RS tasks within broader vision-language foundation models, moving beyond task-specific adaptations to capture general visual-textual representations of Earth observation data across space and time (Li et al., 2024d). GeoChat (Kuckreja et al., 2024) and EarthGPT (Zhang et al., 2024b) adapt LLaVa-style conversational VLMs for RS multi-task reasoning, with GeoChat supporting grounded region-aware dialogue and EarthGPT extending to multi-sensor interpretation and unified RS task handling. RSUniVLM (Liu and Lian, 2024) advances this approach by unifying image-, region-, and pixel-level understanding through a granularity-oriented mixture-of-experts architecture, enabling both fine-grained spatial reasoning and multi-image tasks. UniRS (Li et al., 2024d) further addresses the single-image limitation by introducing a unified spatiotemporal visual representation and a dedicated change-extraction module, allowing a single model to process single images, bi-temporal pairs, and video sequences for comprehensive multi-temporal RS analysis.

Most recently, LLM-driven RS vision-language agents extend these models by integrating perception, reasoning, and tool use into multistep analytical workflows, supporting tasks such as temporal scene understanding and change detection through multi-turn conversations (Irvin et al., 2025; Liu et al., 2024). Tree-GPT is an example of an LLM-driven RS vision-language agent for forest scene analysis. It combines LLM orchestration with knowledge bases, vision understanding modules and a web UI to support interactive forest scene analysis, albeit lacking a temporal component.

2.4. *LLM Agents for Remote Sensing*

AI agents are systems that link perception and action through iterative reasoning to achieve user-defined goals (Xu et al., 2024). Utilising LLMs pretrained on massive text corpora, they can learn from interactions, decompose tasks, and interact dynamically across steps with external data, models, or tools (Liu et al., 2025), serving as suitable modular orchestrators for complex workflow execution (Liu et al., 2024; Schick et al., 2023; Yao et al., 2023; Guo et al., 2024).

Within RS, LLM-based agents are still in their infancy, with applications for Earth observation tasks gradually increasing (Xu et al., 2024; Liu et al., 2024; Du et al., 2023). They are typically task-specific and rely on strict prompt templates and few-shot examples to guide reasoning and improve robustness (Xu et al., 2024; Guo et al., 2024). Agents execute tasks by selecting toolkits that often contain specialised visual modules, which can be run independently or composed into sequential pipelines to accomplish multiple objectives (Guo et al., 2024; Du et al., 2023), as in Change-Agent (Liu et al., 2024) and RS-Agent (Xu et al., 2024). This modular design, which often benefits from integrated knowledge bases and elucidation of task functionalities, helps reduce hallucinations, enhances accuracy, and enables flexible, customisable outputs (Guo et al., 2024; Yao et al., 2023; Liu et al., 2025; Du et al., 2023). RS-specific LLM agents generally fall into two broad paradigms. The first comprises modular tool-using systems that rely on external LLMs to orchestrate specialised vision modules. The second consists of end-to-end instruction-tuned VLMs that embed temporal or multimodal reasoning directly within the model. Recent work illustrates both directions (Liu et al., 2024; Xu et al., 2024; Deng et al., 2025), including hybrid approaches (Irvin et al., 2025).

When introducing ChangeChat - an interactive VLM designed for bi-temporal RS change analysis using multimodal instruction tuning - Deng et al. (2025) claim that approaches such as Change-Agent (Liu et al., 2024) and RS-ChatGPT (Guo et al., 2024), that rely on external LLMs, are limited in end-to-end flexibility, with system capabilities constrained to pre-defined modules. TEOChat (Irvin et al., 2025) bridges the two design philosophies by incorporating instruction tuning over variable length temporal image sequences, enabling stepwise reasoning across multi-date satellite imagery while maintaining modular interpretability. Another prominent limitation raised by Xu et al. (2024) is the challenge of providing flexible task orchestration and mitigating failures in task decomposition reasoning and tool selection, as witnessed with models like RS-Chatgpt (Guo et al., 2024). RS-Agent addresses this by using an LLM as a controller, which parses user instructions, selects from a suite of geospatial tools, and composes multistep workflows. A retrieval-augmented knowledge graph supports the LLM with domain-specific information and task-aware strategies to enable complex reasoning across diverse RS tasks. Change-Agent (Liu et al., 2024), is designed specifically for bi-temporal change analysis, integrating an LLM with change-focused reasoning modules to support interactive and interpretable assessments of temporal differences in RS imagery.

Comparing the capabilities of these various LLM-based RS agents is challenging due to differences in task scope, input modalities, architectural configuration, and evaluation setups. This lack of standardised benchmarking makes it difficult to assess performance, task orchestration, and agentic reasoning across approaches. To date, only ChangeMinds (Wang et al., 2024) and Change-UP (Yang et al., 2025b) benchmark against Change-Agent’s MCI model (Liu et al., 2024) for joint RSCD and RSICC, with both reporting modest gains. However, neither work incorporates an LLM-based agent, or releases code. Other framework either lack temporal reasoning (Guo et al., 2024; Du et al., 2023; Xu et al., 2024), or are limited in their CDC capabilities (Irvin et al., 2025; Deng et al., 2025), leaving Change-Agent as the most appropriate framework identified.

3. Data

3.1. LEVIR-MCI-Trees

When developing the robust MCI model at the heart of the Change-Agent system, Liu et al. (2024) proposed the LEVIR-MCI dataset, which comprises both pixel-level change information contained within change detection masks and descriptive semantic-level captions. Each of the 10,077 examples contains bi-temporal image pairs with a variable time span of 5–15 years, a corresponding annotated mask, and five annotated captions. Each image spans 256×256 pixels at a high spatial resolution of 0.5m/pixel. LEVIR-MCI extends LEVIR-CC (Liu et al., 2022) by providing each pair of bi-temporal images with change detection masks that explicitly highlight changes to roads and buildings, with over 40,000 changed roads and buildings annotated. The five captions for each image pair are intended to provide diverse annotations from varying perspectives to bolster its utility for change detection.

For the purposes of this study, a subset of this dataset was taken that discards image pairs that contain no changes to tree cover, hereby referred to as *LEVIR-MCI-Trees*. Filtering is performed based on the contents of the captions for each example. If none of the captions for an example contains one of: ‘tree, trees, wood, woods, woodland, wooded, forest, forests, jungle, jungles’ then it is removed. Post filtering, the resulting subset contains 2,305 examples distributed across training, validation and test sets comprising 66%, 16% and 18% (1518, 374, 413) of the dataset respectively. Due to the dataset only containing pixel-level annotations for roads and buildings, it is unsuitable for benchmarking Forest-Chat’s performance for deforestation segmentation directly, but can be used to gauge the architecture’s generalisation capabilities to new geographical domains. However, this subset will be suitable for comparing the performance of tree disturbance captioning and highlighting any differences in the difficulty of pixel-level annotation between urban and forest contexts. Segmentation performance in urban settings is generally higher than in natural landscapes due to simpler object geometries and clearer boundaries (Wang et al., 2025), leading to a preference in benchmarking model performance within urban contexts.

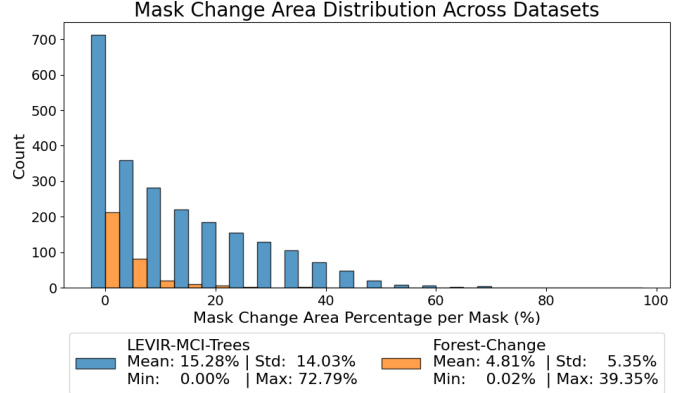


Figure 2: Summary statistics of change cover in segmentation masks for Forest-Change and LEVIR-MCI-Trees datasets.

3.2. Forest-Change

This section outlines the work undertaken to create a novel change caption and detection dataset for forest cover analysis, highlighting the creation process, along with potential limitations.

3.2.1. Data Curation

To the best of our knowledge, no existing benchmark dataset explicitly supports joint forest change detection and captioning (CDC). Lines et al. (2022) highlight the broader scarcity of RS forest monitoring benchmark datasets, and while recent initiatives such as OpenForest (Ouaknine et al., 2025) catalogue available resources, few datasets target forest change specifically.

Among existing datasets, CAM-ForestNet (Debus et al., 2024; Hartanti et al., 2023) is intended to support deforestation segmentation using time-series imagery, providing both change masks and deforestation driver labels. These works largely gather imagery from Google Earth Engine (GEE) and then verify forest cover changes through the open-source Global Forest Watch (GFW) platform (Watch, 2014), which serves as a crucial tool for tracking global forest health. However, it is not designed for joint change detection and captioning tasks, and issues such as misaligned polygons, corrupted or inconsistent imagery, and variable temporal sequences limit its suitability for RSICI model development.

Hewarathna et al. (2024) introduce a dataset focused solely on forest cover change detection, albeit without deforestation driver labels that could support caption generation. It comprises variable-length temporal RGB stacks of tropical and subtropical forest loss from GEE (Gorelick et al., 2017), with a temporal resolution of one year across multiple locations, informed by the WWF Deforestation Fronts report (Taylor et al., 2015). The authors crop, augment, and segment the original images into 480×480 patches at a medium spatial resolution of ~ 30 m/pixel, resulting in 334 annotated bi-temporal image pairs with binary change masks from an original set of 1500.

3.2.2. Preprocessing

Due to overlapping crops and the conversion of temporal image sequences to bi-temporal image pairs, both scene diversity and change mask geometry are limited. As shown in Figure 2, most masks in the Forest-Change dataset contain less than 5% new deforestation, with a maximum of 40%, resulting in a heavily imbalanced dataset that necessitates per-class evaluation rather than global pixel accuracy. In contrast, the LEVIR-MCI-Trees dataset exhibits a higher and more consistent foreground proportion (mean 15.28%, max 72.79%) and more regular object geometries, making change segmentation conceptually easier.

The Forest-Change dataset is organised to mirror the directory structure of LEVIR-MCI-Trees to maintain consistent data loading. Three splits were created for training, validation, and testing at an approximate ratio of 80%:10%:10% (270, 31, and 33 samples, respectively). All images are resized to 256×256 pixels to match LEVIR-MCI-Trees, and pixel-wise change masks are binarised to indicate change (1) or no-change (0). The bi-temporal image pairs are pre-aligned, and no additional geometric registration or atmospheric correction was applied. Images were normalised using dataset-specific per-channel mean and standard deviation statistics. No additional radiometric correction or cloud masking was performed, although a few samples exhibit partial cloud occlusion.

3.2.3. Caption Generation

As shown in Figure 2, captions for the Forest-Change dataset are skewed toward descriptions of lower degrees of forest loss and recurring loss patterns. This reflects the limited scene diversity introduced by the cropping-augmentation strategy adopted by [Hewarathna et al. \(2024\)](#), as discussed previously in Section 3.2.1. Captioning extensive amounts of remote sensing change imagery is fatiguing for human annotators, especially when underlying scene diversity is limited. Therefore, rule-based caption generation is proposed as a way to ensure minimal requirements for adequate semantic context and sentence structure are met. Human annotations are still valuable for improving linguistic and semantic variation, and providing geographic context.

Caption generation was conducted using a two-stage approach combining manual annotation with rule-based caption synthesis. A custom Streamlit-based application was developed to facilitate captioning due to its suitability for rapid interactive prototyping and its prior integration within the Change-Agent framework ([Liu et al., 2024](#)).

The application prompts the user to select a dataset directory, following the LEVIR-MCI-Trees' folder structure (also used for Forest-Change). Previously labelled samples can be skipped to support incremental annotation. The annotator is iteratively presented with bi-temporal image pairs and the corresponding change mask, and asked to provide a single short-to-moderate length caption describing the observed change. Upon submission, four additional captions are automatically generated based

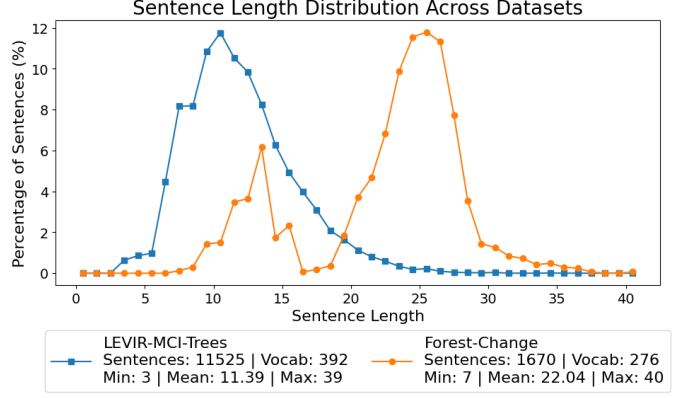


Figure 3: Summary statistics of captions for Forest-Change and LEVIR-MCI-Trees datasets.

on properties extracted from the change mask - producing a total of five captions.

For automated caption generation, the percentage of newly deforested area, the size of individual change patches, and their spatial distribution are computed from the mask. The percentage of forest loss is binned into adjective-based descriptors aligned with the model vocabulary. A rule-based caption generator was designed to introduce lexical and syntactic variation, producing complementary captions to the human-provided description. Although LLMs are increasingly used for synthetic text generation in NLP tasks [Yu et al. \(2023\)](#), they were not adopted here due to the risk of introducing prompt-induced bias and the limited scope of the project in which to mitigate it.

Figure 3 compares caption characteristics between Forest-Change and LEVIR-MCI-Trees. Captions in LEVIR-MCI-Trees are generally shorter and exhibit greater lexical diversity, while Forest-Change captions display a bimodal length distribution that reflects the combination of rule-based and human-generated annotation. By combining the unique characteristics of the datasets, evaluating model performances becomes more robust. Figure 4 presents representative caption examples from the Forest-Change dataset, illustrating the range of forest loss descriptions.

4. Methodology

This section outlines the components of the Forest-Chat agent. The goal of the Forest-Chat agent is to provide a conversational interface for bi-temporal remote sensing (RS) forest change analysis through joint pixel-level change detection and change captioning (CDC). Building on the Change-Agent framework ([Liu et al., 2024](#)), Forest-Chat integrates a domain-specific VLM (the MCI model) for supervised CDC, a zero-shot foundation vision model (AnyChange) for class-agnostic pixel-level change localisation, and an LLM controller for instruction interpretation, tool selection, and analytical reasoning. To adapt Forest-Chat for forest change analysis, the

(a) three noted areas of loss in the top left top right and centre on the edge of previous clearings new loss is moderate whilst overall loss is considerable



(b) slight forest degradation is noted scattered across multiple regions occurring in many small patches which are highly varied in size



(c) some modest forest loss is detected largely concentrated in the top-left and top-center sections occurring in many small patches which are displaying large variations in size



(d) minor forest loss is visible occurring in many small patches which are showing some variation in size mainly located in the top-left area



Figure 4: Four examples from the Forest-Change dataset, that each display a randomly selected caption, combined with image A, image B, and the corresponding forest change mask.

MCI model is trained on the Forest-Change and LEVIR-MCI-Trees datasets to produce structured change masks and semantic change descriptions. When used in a supervised capacity, the system is referred to as FC-Supervised. The system is further augmented with the AnyChange model to enable zero-shot change detection on out-of-distribution data, with this capability termed as FC-Zero-shot. To support interactive zero-shot change analysis, an interface is developed for user-provided point prompts to guide object-oriented change detection with AnyChange. Finally, the Forest-Chat toolset is extended with forest-specific analytical functions, including deforestation area estimation and patch-level statistics, enabling both low-level perception and high-level reasoning within a unified agentic framework.

The overall system diagram for Forest-Chat is presented in Figure 1, while Figure 5 provides a simplified overview of the per-

ception models incorporated into Forest-Chat. The components of Forest-Chat are described below.

4.1. Multi-level Change Interpretation Model

The MCI model is a dual-branch VLM designed to process pairs of bi-temporal RS images, as shown in Figure 5a. It employs a Siamese SegFormer B1 backbone (Xie et al., 2021) to extract multi-scale semantic features from each image, providing both low-level detail and high-level contextual information. These features form the shared representation from which two task-specific branches are derived.

Bi-temporal Iterative Interaction (BI3) layer: A central innovation of the MCI model that is embedded within the change detection and change captioning branches, which aims to enhance and fuse bi-temporal features. It combines two modules: *Local Perception Enhancement* (LPE), and *Global Difference Fusion Attention* (GDFA) to extract discriminative features of interest.

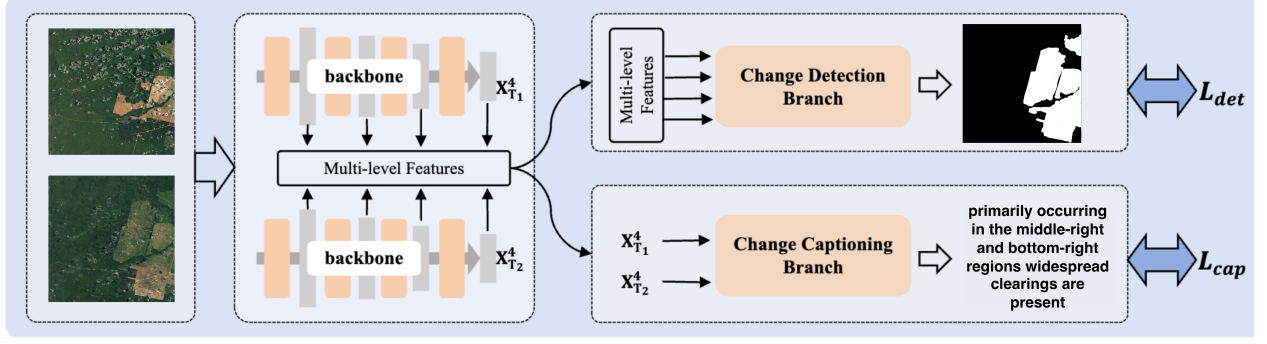
The LPE module applies convolutions of different kernel shapes to capture variations across multiple spatial scales, producing feature maps that enrich the diversity of feature information and the ability to detect local changes. Subsequently, the GDFA module uses feature differencing and attention to highlight regions of true change while down-weighting irrelevant noise. Following the LPE and GDFA modules, Layer Normalisation (LN) and a Multi-Layer Perceptron (MLP) are applied to the bi-temporal features to enhance them. Stacking BI3 layers across the branches progressively strengthens feature discrimination. This implementation uses a total of three BI3 layers per branch.

Change detection branch (top right, Fig. 5a): Applies stacked BI3 layers with residual connections to iteratively enhance and refine the high-level bi-temporal features extracted from the backbone. This improves the model’s capacity to capture meaningful semantic differences between time points. To recover finer spatial detail, the branch then employs Convolution-Based Bi-temporal Fusion (CBF) modules across four spatial scales to give four window sizes, progressively integrating features from both images. Finally, a deconvolution pathway merges these multi-scale representations from bottom to top, enabling the production of precise, high-resolution change masks.

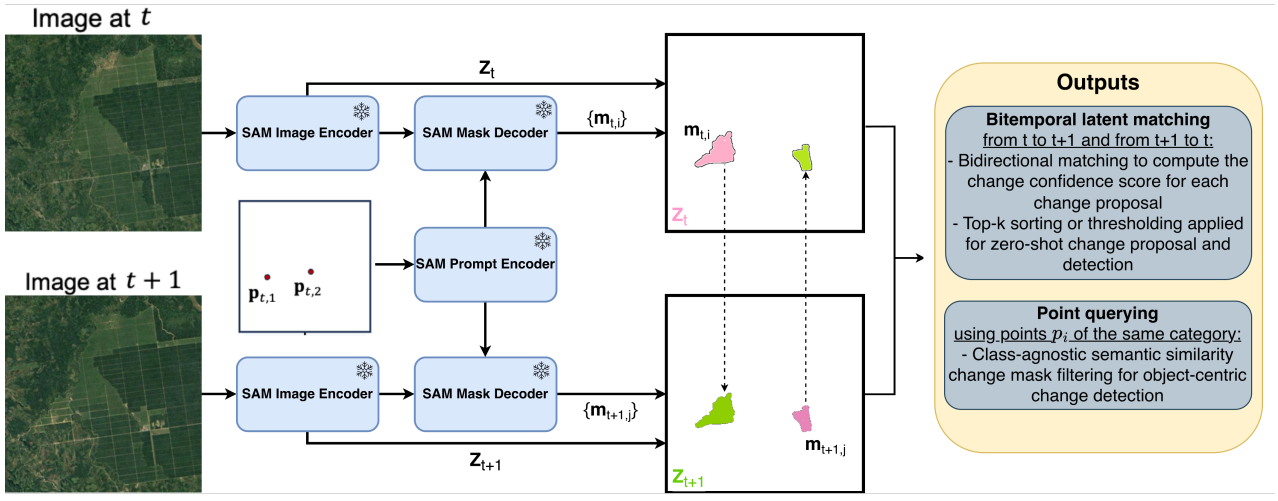
Change captioning branch (bottom right, Fig. 5a): Addresses semantic-level interpretation, transforming vision differences into natural language descriptions. It begins with multiple stacked BI3 layers, which refine and align high-level semantic features from the bi-temporal images. These enhanced features are then passed through a convolution-based projection layer, bridging the visual and textual domains. Finally, the projected features are decoded by a Transformer decoder operating with a 512-dimensional word embedding space, generating descriptive sentences of the observed changes.

4.2. LLM Agent Task Orchestration

The LLM functions as the controller of Change-Agent (Fig. 1 right side), directing task execution and dynamically respond-



(a) MCI model overview. Adapted from ChangeAgent (Liu et al., 2024).



(b) AnyChange overview.

Figure 5: Overview of the two visual perception models available to the Forest-Chat agent. (a) highlights the overall structure of the MCI model (b) introduces a simplified overview of the AnyChange model.

ing to user queries. While some recent LLMs are equipped with native visual perception (openai et al., 2023), these capabilities are not yet optimally suited to RS imagery, which requires specialised feature extraction (Zhang and Wang, 2024). To address this, the system is extended with Python-based tools, including the backbone feature extractor, change detection and change captioning modules, and standard processing libraries. By generating and executing Python programs, the LLM can invoke these tools as needed, enabling automated multistep workflows without human intervention. Within the application interface, users are able to apply and remove tools as desired, including access to Google Scholar and Google Search for external knowledge. It is within the change perception module that the AnyChange (Zheng et al., 2024) model and additional forest change specific functions are made available to the central LLM, realising the idea of Forest-Chat.

In this framework, *ChatGPT-4o-mini* serves as the LLM backbone, selected to balance performance, speed, and cost. The system is capable of incorporating alternative LLMs (e.g. *InternLM2.5-7B-Chat* (Cai et al., 2024)) for task orchestration and execution, with selection predominantly based on the degree of complex reasoning required or availability of computing

power. After processing tool outputs, the LLM synthesises results into natural language responses, whether as change masks, descriptive captions, object counts, deforestation percentages, predictive assessments, and causal reasoning. System prompts with few-shot examples are provided to the LLM to support forest change analysis workflows, ensuring reliable tool invocation and consistent output formatting. This enables the combination of detailed and grounded visual analysis with flexible reasoning and user-facing interaction.

4.3. AnyChange for Zero-shot Change Detection

The AnyChange model developed by Zheng et al. (2024) introduces a training-free framework for zero-shot change detection for RS imagery (Fig. 1 lower left, Fig. 5b). The method builds on the Segment Anything Model (SAM) (Kirillov et al., 2023), adapting its latent space for bi-temporal analysis without requiring fine-tuning. The model is designed to generalise across unseen change types and data distributions, producing either pixel-level or instance-level predictions. It supports three modes of operation: fully-automatic, semi-automatic (threshold-based), and prompt-guided using point inputs.

The approach is grounded in the structured properties of SAM’s latent space. Mask embeddings generated by the image encoder provide semantic information such that objects of the same category (e.g. water, buildings, bare land) cluster together within a single image. Furthermore, corresponding object categories across temporally separated images of the same location remain closely aligned despite differences in imaging conditions (e.g. seasonality). These intra-image and inter-image semantic consistencies provide the foundation for adapting SAM to RSCD without retraining or architectural modifications.

AnyChange employs a bi-temporal latent matching strategy in which object masks are first generated for each temporal image using SAM, and embeddings for each mask are computed by averaging the corresponding image encoder inputs. The semantic similarity between embeddings is quantified using a cosine-based metric, allowing changes to be identified as deviations between corresponding object embeddings over time. The method ensures temporal symmetry by performing bidirectional matching between time points. Change predictions can then be obtained either by ranking confidence scores or applying a threshold on embedding angles.

To enable object-centric change detection, AnyChange combines its bi-temporal latent matching with SAM’s point prompt mechanism, yielding a *point query mechanism*. Users provide a set of spatial coordinates on a single-temporal image, which are treated as point prompts corresponding to a specific category. SAM generates object proposals for these points, and the average mask embeddings are computed. These embeddings are then matched with proposals from both temporal images using cosine similarity, producing change scores that can be filtered using a user-defined angle threshold provided by the bi-temporal latent matching approach.

Instead of inputting a list of point coordinates, this paper develops an interactive application interface that allows users to click directly on areas of interest to generate point queries, improving convenience over manual coordinate entry.

4.4. Multi-task Loss Balancing Strategy

During the training of the MCI model, multi-task learning is performed on both change detection and change captioning. For both tasks, standard cross-entropy loss is used to quantify the dissimilarity between predicted change masks and ground truth annotations, and the dissimilarity between predicted sentences and their corresponding ground truth sentences respectively. The two losses have significant discrepancies between their magnitudes, which negatively impacts overall change interpretation performance, due to the risk of one task dominating the training signal of the other. A common approach, which is used by Liu et al. (2024), and consequently adopted here, is to normalise the losses to the same order of magnitude and detach their gradients for stability. This ensures that each task contributes equally to the final loss function, and enables a simultaneous optimisation of the dual change detection and captioning tasks. The final loss function is derived as:

$$\mathcal{L}_{\text{total}} = \frac{\mathcal{L}_{\text{det}}}{\text{detach}(\mathcal{L}_{\text{det}})} + \frac{\mathcal{L}_{\text{cap}}}{\text{detach}(\mathcal{L}_{\text{cap}})} \quad (1)$$

where $\text{detach}(\cdot)$ denotes the operation to detach the gradient, \mathcal{L}_{det} is the change detection cross-entropy loss, and \mathcal{L}_{cap} is the change captioning cross-entropy loss.

4.5. Evaluation Metrics

To evaluate the performance of Forest-Chat’s supervised and zero-shot settings for binary change detection in remote sensing images, the Mean Intersection over Union (MIoU) metric is employed. MIoU quantifies segmentation quality by measuring the average overlap between predicted change masks and ground-truth masks across all classes. MIoU is defined below as:

$$\text{MIoU} = \frac{1}{C} \sum_{i=1}^C \frac{TP_i}{TP_i + FP_i + FN_i} \quad (2)$$

where C is the number of classes (i.e. change (c), no change (nc) for which metrics are calculated. For each class i , TP_i are true positives, FP_i false positives, and FN_i false negatives for class i .

By analysing both the individual class performances through IoU, as well as MIoU, model predictions for the under-represented change class can be compared. Overall accuracy (OA) is naturally a poor performance indicator for this task due to the severe class imbalances present in both datasets. Despite LEVIR-MCI-Trees containing three classes (i.e. road, building, background), performance metrics are calculated on the basis of *change* (c) and *no change* (nc), harmonising the results with those obtained for Forest-Change.

For evaluating the change captioning capabilities of FC-Supervised, the evaluation metrics employed by Liu et al. (2024) are re-used here for consistency. The four metrics are redefined here:

- **BLEU-n** (Papineni et al., 2002): Measures n-gram similarity between generated and reference sentences. Evaluated for n-grams of size 1 to 4, producing a total of four BLEU scores. Shortened to Bn in tables for readability.
- **METEOR** (Banerjee and Lavie, 2005): Calculates the harmonic mean of unigram precision and recall, incorporating a penalty mechanism to assess generated sentence fluency.
- **ROUGE_L** (Lin, 2004): Measures similarity based on the longest common subsequence between generated and ground-truth sentences, prioritising recall performance for evaluating longer captions.
- **CIDEr-D** (Vedantam et al., 2015): Computes cosine similarity between Term Frequency Inverse Document Frequency (TF-IDF) weighted n-gram vectors, treating each caption as a document to assess the semantic relevance.

Through these metrics, a comprehensive assessment of both change detection and captioning can be performed. By including per-class segmentation performance metrics, a deeper understanding of the under-represented *change* class can be obtained. Across all metrics, higher scores indicate better change masks or improved sentence quality.

5. Experiments

5.1. Experimental Setup

All models are implemented in PyTorch and trained via CPU on Isambard 3 (Green et al., 2025), demonstrating that high computational resources are not required. Inference time benchmarking is conducted via CPU on an Apple M3 Pro. The maximum number of epochs is set to 100, with the backbone being trained until the sum of the MIoU and BLEU-4 scores does not improve for 10 consecutive epochs on the validation set. For FC-Supervised, once trained, the backbone network is subsequently frozen, and training is continued on the best model for the two branches separately. When training, the goal is to minimise the loss function defined in Equation 1, utilising the Adam optimiser with an initial learning rate of 0.0001.

5.2. Forest-Chat Supervised Performance

There remains a lack of available methods that provide simultaneously capabilities for joint change detection and captioning (CDC). Consequently, performance evaluations are done by comparing FC-Supervised to SOTA models for the two tasks separately on the LEVIR-MCI-Trees and Forest-Change datasets. Change3D (Zhu et al., 2025) is capable of both tasks, but is not implemented in a unified manner. BiFA (Zhang et al., 2024a) is selected for change detection, and Chg2Cap (Chang and Ghamisi, 2023) for change captioning. Additionally, identifying differences in difficulty between the two datasets can be addressed, comparing performances in a low-data forest change analysis scenario against a more urban focused one constructed from a larger and more varied dataset.

Table 1 provides the performance comparisons for the benchmarked models on both datasets. For both datasets, FC-Supervised is the strongest performer for change captioning, and is the best on LEVIR-MCI-Trees for change detection. On the Forest-Change dataset, FC-Supervised is marginally outperformed by BiFA Zhang et al. (2024a) for change class identification, with both models achieving similar overall performance. These results demonstrate strong generalisation capabilities across varying data domains for both change detection and captioning. Among the benchmarked methods, FC-Supervised is the slowest at captioning inference and the second slowest for change detection (see Table 2). This is expected because it performs joint multi-task reasoning with heavy cross-modal and cross-temporal interactions and multi-task attention. However, these inference times are not prohibitive for practical applications, especially given that only a single model is required to generate pixel-level and semantic-level information of changes within RS image pairs. Zero-shot inference times are discussed in the next section.

Overall change detection performance is considerably better for building and road detection than for deforestation, likely due to the pronounced class imbalances within Forest-Change, fuzzy edges at the borders of many deforestation patches, the uniqueness of deforestation patterns, and the relatively small dataset size. Within the Forest-Change dataset, a considerable percentage of change masks are comprised of numerous tiny patches that are challenging for models to detect. Correspondingly, this resulted in all benchmarked CD models frequently predicting change masks that mirrored the deforestation patterns observed, but contained few overlaps with the ground-truth masks (see row 4 in Fig. 6). Models generally perform well on larger patches, but would still struggle with accurately predicting fuzzy boundaries. This corroborates the findings of Liu et al. (2024), who highlight the segmentation performance of objects containing fewer than 400 pixels is low. Compared with deforestation detection, building change detection patterns and object geometries are more predictable, further raising the challenge posed by the Forest-Change dataset.

Captioning performance evaluation is more nuanced. For the LEVIR-MCI-Trees dataset, the BLEU-1, BLEU-2, and CIDEr-D metrics are generally higher, while BLEU-3, BLEU-4, METEOR, and ROUGE_L are better for Forest-Change. The observed results largely reflect the differences in annotation styles between the two datasets, as described in Section 3.2.3. Despite models frequently predicting deforestation severity accurately, they occasionally get confused about the location and characterisation of deforestation patches, and are unable to recognise geographic features within the imagery. Improved caption generation, or domain-aware approaches, such as vocabulary expansion (Gao et al., 2024) or domain-adaptive fine-tuning (Guo et al., 2022), could mitigate this by elevating the representation of geophysical descriptors in the latent space of these models.

5.3. Forest-Chat Zero-shot Performance

In keeping with the previous section, FC-Zero-shot performance is evaluated on both the Forest-Change and LEVIR-MCI-Trees datasets. To optimise performance, a Bayesian hyperparameter search comprising 20 runs was conducted to identify the most influential parameters. Following the Segment Any Change framework (Zheng et al., 2024), bi-temporal matching and feature normalisation are enabled throughout due to their consistently positive impact on change discrimination.

The following hyperparameters are tuned:

- **Change confidence threshold:** Specifies the minimum cosine distance in the latent feature space required to classify a region as changed, directly governing the trade-off between sensitivity and false positives.
- **Stability score threshold:** Filters mask proposals based on their consistency under point prompt perturbations, suppressing unstable or noisy change predictions.

Table 1: Change Detection and Change Captioning performances on the test sets of LEVIR-MCI-Trees and Forest-Change datasets. Best results per dataset and metric are **bold**, second-best are underlined. Results are an average of three runs.

Dataset	Model	MIoU	IoU_{nc}	IoU_c	B1	B2	B3	B4	METEOR	ROUGE _L	CIDEr-D
LEVIR-MCI-Trees	BiFA	<u>87.54</u>	<u>95.63</u>	<u>79.45</u>	-	-	-	-	-	-	-
	Chg2Cap	-	-	-	70.25	53.88	38.56	27.28	21.80	45.65	37.72
	Change3D	87.48	<u>95.63</u>	79.34	69.52	<u>54.35</u>	38.33	26.41	21.57	<u>46.83</u>	35.03
	FC-Supervised	88.13	95.89	80.36	75.25	60.90	46.21	34.41	23.32	49.34	48.69
Forest-Change	BiFA	67.34	95.85	38.84	-	-	-	-	-	-	-
	Chg2Cap	-	-	-	59.09	45.12	34.59	27.10	23.50	43.41	12.97
	Change3D	66.01	<u>95.93</u>	36.08	61.08	49.18	40.46	<u>33.32</u>	<u>25.65</u>	<u>46.26</u>	20.78
	FC-Supervised	<u>67.10</u>	96.12	38.07	67.54	56.34	47.55	40.17	28.22	48.52	38.79

Table 2: Inference time per iteration (s), averaged across both datasets.

Task	Model	Time / iter (s)
Change Captioning	Change3D	4.00
	Chg2Cap	3.81
	FC-Supervised	5.35
Change Detection	Change3D	0.53
	BiFA	0.84
	FC-Supervised	1.84
	FC-Zero-shot	31.88

- Area threshold:** Suppresses small or fragmented change regions by enforcing a minimum relative area requirement, helping reduce spurious detections in cluttered scenes.
- Object similarity threshold:** Regulates the tolerance for matching corresponding regions across temporal images, influencing the balance between over-segmentation and missed change instances.

The remaining hyperparameters are not tuned due to their minimal impact on mask generation. Points-per-side - which controls the spatial density of point prompts provided to SAM for mask proposal generation - is fixed at 16 as a practical trade-off between performance and run-time. Performing a full hyperparameter sweep on LEVIR-MCI-Trees is computationally prohibitive, so the best configuration from Forest-Change is reused. These parameters mainly control proposal density and filtering heuristics, rather than dataset-specific semantics, so reusing them is unlikely to introduce systematic bias.

Table 3 provides an overview of FC-Zero-shot’s change detection performance. Of the hyperparameters, the change confidence threshold was found to have the highest influence on performance. Overall, the optimal hyperparameters differed minimally from those found by Zheng et al. (2024), with performance increases of 0.95% MIoU and 9.28% on the Forest-Change and LEVIR-MCI-Trees datasets respectively. Zero-shot performance is noticeably lower on both datasets when compared to the supervised methods, but the discrepancy is much more pronounced for LEVIR-MCI-Trees. This can be

partly attributed to the segmentation masks only containing annotations for road and building changes, so any other identified changes will be penalised during evaluation. Additionally, FC-Supervised has a stronger supervision signal on the LEVIR-MCI-Trees dataset due to better image quality and variety, resulting in higher segmentation quality. A visual comparison between the various benchmarked methods on the Forest-Change dataset is provided in Figure 6.

Generally, FC-Zero-shot is highly sensitive to atmospheric artifacts and seasonal change, resulting in frequent cases of false positives. This sensitivity can potentially be mitigated by providing point queries. However, point queries are best utilised when segmenting over multiple object classes, as compared to the binary case presented by Forest-Change. Besides, there is no methodological process for determining the optimal placement of point queries. However, the development of an interactive interface that enables users to provide point queries is a useful contribution for faster investigations into optimal point prompt placements.

Table 3: FC-Zero-shot segmentation performance with default parameters and best hyperparameter sweep configuration. Best configuration: change confidence threshold = 145; stability score threshold = 0.93; area threshold = 0.9; object similarity threshold = 60.

Dataset	Model	MIoU	IoU_{nc}	IoU_c
Forest-Change	FC-Zero-shot ^D	58.56	93.83	23.29
	FC-Zero-shot ^B	59.51	94.64	24.38
	FC-Supervised	67.10	96.12	38.07
LEVIR-MCI-Trees	FC-Zero-shot ^D	38.04	54.05	22.04
	FC-Zero-shot ^B	47.32	66.60	28.04
	FC-Supervised	88.13	95.89	80.36

^D Default parameters; ^B Best hyperparameter configuration.

Despite lowering the points-per-side hyperparameter, inference time is still significantly slower than all other benchmarked methods, as shown in Table 2. FC-Zero-shot runs the SAM image encoder on each image, using a ViT-h as the default backbone, resulting in extensive inference times. Reducing the ViT size would speed up inference, but compromise performance, which is already a limiting factor to practical applications. While this approach is capable of outperforming pre-VLM su-

pervised change detection approaches (e.g. (Hewarathna et al., 2024)), and has the ability to detect changes that may have been missed by human annotators, it lags behind contemporary supervised methods and is sensitive to atmospheric noise and seasonal variations. Future work in this area could focus on extending SAM’s (Kirillov et al., 2023) textual prompting to change detection, or accounting for challenges inherent to RS imagery, something that the underlying SAM model is not designed for due to pre-training focusing on natural images. Comparing alternative remote sensing-pretrained foundational vision backbones would be valuable for aligning extracted features with change mask proposals.

5.4. Balancing Change Detection and Captioning Study

While normalised loss balancing is effective at preventing one task from dominating the learning gradient, it statically assumes that tasks are equally important and difficult throughout training, potentially ignoring the fundamental noise heteroscedasticity between tasks. To investigate this, we experiment with various multi-task learning (MTL) loss balancing and gradient normalisation techniques to assess their impact on the joint training of CDC and their potential to improve collaborative learning.

For MTL loss balancing, we select Uncertainty Weighting (Kendall et al., 2018) and Enhanced Dynamic Weight Averaging (EDWA) (Shi et al., 2024). For gradient conflict resolution, we evaluate Conflict-Averse Gradient Descent (CAGrad) (Liu et al., 2021), Projecting Conflicting Gradients (PCGrad) (Yu et al., 2020), and GradDrop (Chen et al., 2020). These methods are also combined in various configurations to form a comprehensive experimental suite capable of detecting any combinations that produce notable performance differences.

Experiments are performed only on the smaller Forest-Change dataset due to computational limitations. Due to the stochastic nature of the full experimental results presented in Tables A.1 and A.2, the results for each method are aggregated and presented in Table 4. The results show clearly that the optimum strategy previously found of normalising the losses against each other remains the best approach for balancing the two tasks. This suggests that the FC-Supervised’s learning objectives are naturally aligned, and that the architecture already provides sufficient task decoupling. Although the captioning loss exhibits larger numerical values than the change detection loss, equal task weighting and no gradient conflict resolution generally yields superior performance. This suggests that loss magnitude alone is not indicative of effective gradient influence. In practice, the dense spatial supervision of change detection produces strong and stable gradients that naturally balance the higher-variance sequence loss from captioning. In these circumstances, dynamic loss balancing and gradient conflict resolution largely introduce unnecessary optimisation noise, potentially disrupting beneficial cross-task regularisation. Uncertainty weighting is the only approach that marginally improves some captioning metrics, but at a cost to segmentation. These results validate the efficacy of a joint learning framework for

RSCDC, with future work likely to benefit from designing better model architectures and training strategies enhanced task performance.

5.5. FC-Supervised Backbone Size Influence

This section reports on the importance of the Segformer backbone model for feature extraction on downstream tasks. By default, a MiT-B1 is used, but this study tests change detection and captioning performance when using the B0 and B2 sizes. Due to computational limitations and the diminishing returns observed in the original Segformer paper (Xie et al., 2021), backbone sizes above B2 are not explored in this study. Table 5 clearly displays a trend of increasing performance in change detection for both datasets as the backbone size increases. FC-Supervised with the MiT-B2 backbone is shown to be the best change detection model across both datasets, with greater backbone sizes driving improved change class identification. On the Forest-Change dataset, the Mit-B2 backbone outperforms BiFA (Zhang et al., 2024a) in Table 1, making FC-Supervised the best performing model when using a larger backbone. Beyond MiT-B1 though, overall performance gains begin to diminish on both tasks, and even recede for change captioning, indicating that the features extracted by larger backbone predominantly benefit the change detection task more. Training times also grow exponentially, limiting the usage of backbones beyond MiT-B2. Despite slower inference times, FC-Supervised with the MiT-B2 backbone trains at a speed comparable to the benchmark models from Section 5.2, highlighting the efficiency of the architecture’s dual-training approach. These results indicate that backbones need to be carefully selected based on the ability to extract features equally useful to both tasks - especially from models with fewer parameters to improve practical usage.

5.6. Forest-Chat as a Tool for Forest Change Analysis

To qualitatively assess benchmark model performance on the Forest-Change dataset, Figure 6 presents representative examples of change mask and change caption predictions from their respective task capable models. For change mask generation, all change detection capable methods are capable of capturing larger and medium change areas, with the FC-Supervised the most accurate for smaller change regions. All models struggle with accurately predicting numerous small, scattered change regions. When used in a zero-shot capacity, Forest-Chat is notably more susceptible to producing false positives (red), with extreme sensitivity to atmospheric noise. Like the supervised methods, it is capable of detecting the main regions and patterns of change, but often has little overlap when encountering small scattered loss patterns. Smoother change boundaries and spatial coherence are observed for both supervised and zero-shot settings in Forest-Chat compared to the other benchmarked methods, likely due to attention-based feature aggregation and region-level decoding.

For generating change captions describing forest change, only FC-Supervised is able to construct sentences that reliably include semantic information denoting change severity, location,

Table 4: **Aggregated change detection and change captioning performance for MTL strategies on the Forest-Change dataset.** Mean \pm standard deviation across configurations, with three runs each. Bold indicates the best mean value per metric within each group when the improvement is clearly distinguishable relative to standard deviation

MTL Strategy	Method	MIoU	IoU_{nc}	IoU_c	B1	B2	B3	B4	METEOR	$ROUGE_L$	CIDEr-D
Loss Balancing	Equal	67.34\pm0.44	96.20 \pm 0.12	38.47\pm0.85	64.68\pm3.95	53.88 \pm 4.12	45.33 \pm 4.41	38.43 \pm 4.52	27.55 \pm 1.87	47.55 \pm 2.74	35.57\pm8.53
	EDWA	66.88 \pm 0.70	96.19 \pm 0.20	37.56 \pm 1.35	64.46 \pm 4.47	53.69 \pm 4.29	44.78 \pm 4.36	37.73 \pm 4.53	27.47 \pm 2.60	47.71 \pm 3.21	33.13 \pm 6.35
	Uncertainty	67.02 \pm 0.55	96.22 \pm 0.31	37.83 \pm 0.95	63.89 \pm 3.41	53.88 \pm 3.49	45.65 \pm 3.69	39.10\pm4.03	27.95\pm2.15	48.67\pm2.90	33.74 \pm 8.09
Gradient Conflict Resolution	None	67.23\pm0.34	96.24 \pm 0.23	38.22\pm0.53	66.00\pm4.37	55.51\pm3.75	46.99\pm3.57	40.05\pm3.67	28.34\pm2.41	48.73\pm3.16	36.84\pm9.95
	CAGrad	67.16 \pm 0.53	96.26 \pm 0.16	38.06 \pm 0.92	63.68 \pm 2.49	53.49 \pm 3.06	45.47 \pm 3.69	39.00 \pm 4.22	27.77 \pm 1.26	48.40 \pm 1.98	35.05 \pm 6.47
	PCGrad	66.87 \pm 0.70	96.19 \pm 0.13	37.54 \pm 1.42	64.39 \pm 3.71	53.72 \pm 3.57	44.95 \pm 3.58	38.13 \pm 3.84	27.25 \pm 2.10	47.15 \pm 2.60	35.03 \pm 5.31
	GradDrop	67.05 \pm 0.75	96.11 \pm 0.31	37.99 \pm 1.39	63.29 \pm 4.64	52.54 \pm 4.91	43.60 \pm 5.14	36.48 \pm 5.13	27.25 \pm 2.83	47.62 \pm 3.84	29.65 \pm 6.97

Table 5: Change Detection and Change Captioning performances on the test sets of LEVIR-MCI-Trees and Forest-Change datasets using different Segformer backbone sizes for FC-Supervised. Best results per metric are **bold**, second-best are underlined. The training time is reported as a rounded mean \pm standard deviation (s) for a single epoch. Results are averages of three runs.

Dataset	Backbone	MIoU	IoU_{nc}	IoU_c	B1	B2	B3	B4	METEOR	$ROUGE_L$	CIDEr-D	Training Time (s)
LEVIR-MCI-Trees	MiT-B0	87.12	<u>95.52</u>	78.72	72.09	57.76	42.68	31.03	22.73	48.98	42.63	592 \pm 2.52
	MiT-B1	<u>88.13</u>	<u>95.89</u>	<u>80.36</u>	75.25	60.90	46.21	34.41	<u>23.32</u>	<u>49.34</u>	48.69	1437 \pm 27.39
	MiT-B2	88.62	96.03	81.20	<u>74.67</u>	<u>60.63</u>	<u>45.90</u>	<u>34.10</u>	23.61	49.83	<u>48.31</u>	2910 \pm 3.61
Forest-Change	MiT-B0	65.86	<u>96.16</u>	35.55	61.17	50.40	41.46	34.56	26.93	46.76	27.04	256 \pm 1.00
	MiT-B1	<u>67.10</u>	96.12	<u>38.07</u>	67.54	<u>56.35</u>	<u>47.55</u>	<u>40.17</u>	<u>28.22</u>	<u>48.52</u>	<u>38.79</u>	419 \pm 1.53
	MiT-B2	68.01	96.35	39.67	<u>67.25</u>	57.44	49.63	43.23	30.19	51.94	44.15	986 \pm 12.50

and patch characteristics. Of these descriptors, it is most consistent with severity. When describing the locality and patchiness, the caption quality can be seen to occasionally degrade, such as with examples 1, and 4. Both Change3D and Chg2Cap routinely exhibit issues with providing sufficient semantic detail and well-formed sentence compositions. Due to training performances optimising against BLEU-4, all models have learnt to replicate the rule-based generation inherent to the majority of the captions within the training dataset, almost entirely ignoring the semantic language provided by the human captions. Generally, the caption quality is encouraging, but all models will require stronger training data and domain-aware learning to improve lexical richness and geographic domain grounding.

Figure 7 presents two representative conversations with the Forest-Chat agent, which incorporates the supervised change interpretation, zero-shot change detection, additional tooling, and a ChatGPT-4o-mini instance for task orchestration and interaction. The conversations highlight the agent’s ability to respond to user queries through natural language and provide appropriate information according to the request. Demonstrated within the conversation is the ability to produce change masks via supervised and zero-shot methods, provide descriptive change captions, estimate the percentage of area affected by deforestation, count the number of cleared patches, and reason about future change. The agent provides this rich degree of interaction and analysis through a combination of its innate knowledge and the toolset provided to it.

In line with claims made by Xu et al. (2024), the overall toolset available to the agent is small, and new functionality needs to be manually incorporated into the agent, with few-shot examples

helping to guide its awareness of how to utilise the tool. Additionally, the agent would periodically fail to construct valid executable Python code, or get confused about how to respond to the user’s request. This can occur due to the limited support that few-shot examples provide, since they may not adequately cover an expanding range of supported tasks. Providing a task-aware retrieval strategy that can access predefined task solutions, can significantly improve the utilisation of toolsets (Xu et al., 2024).

6. Discussion and Future Work

The development of Forest-Chat demonstrates the feasibility of adapting VLMs with conversational interfaces for forest change analysis. The system can generate both pixel-level change masks and semantic captions that allow users to explore temporal dynamics interactively. The system effectively identifies dominant and visually salient change patterns, demonstrating the value of aligning visual interpretation with natural language interaction. At the same time, the results highlight two important remaining challenges: detecting small, spatially fragmented forest change patches, and identifying visually subtle but ecologically significant changes.

Compared with other datasets for RSCDC, Forest-Change exhibits notable limitations in terms of scale and diversity. The RS imagery and change masks are derived from a limited number of unique sites (Hewarathna et al., 2024). Additionally, the generation of the majority of captions via a programmatic approach compounded by the limited mask diversity resulted in suboptimal caption quality and an artificial limitation in linguistic complexity that largely ignores each scene’s geographical context. Developing a large, diverse forest change dataset with

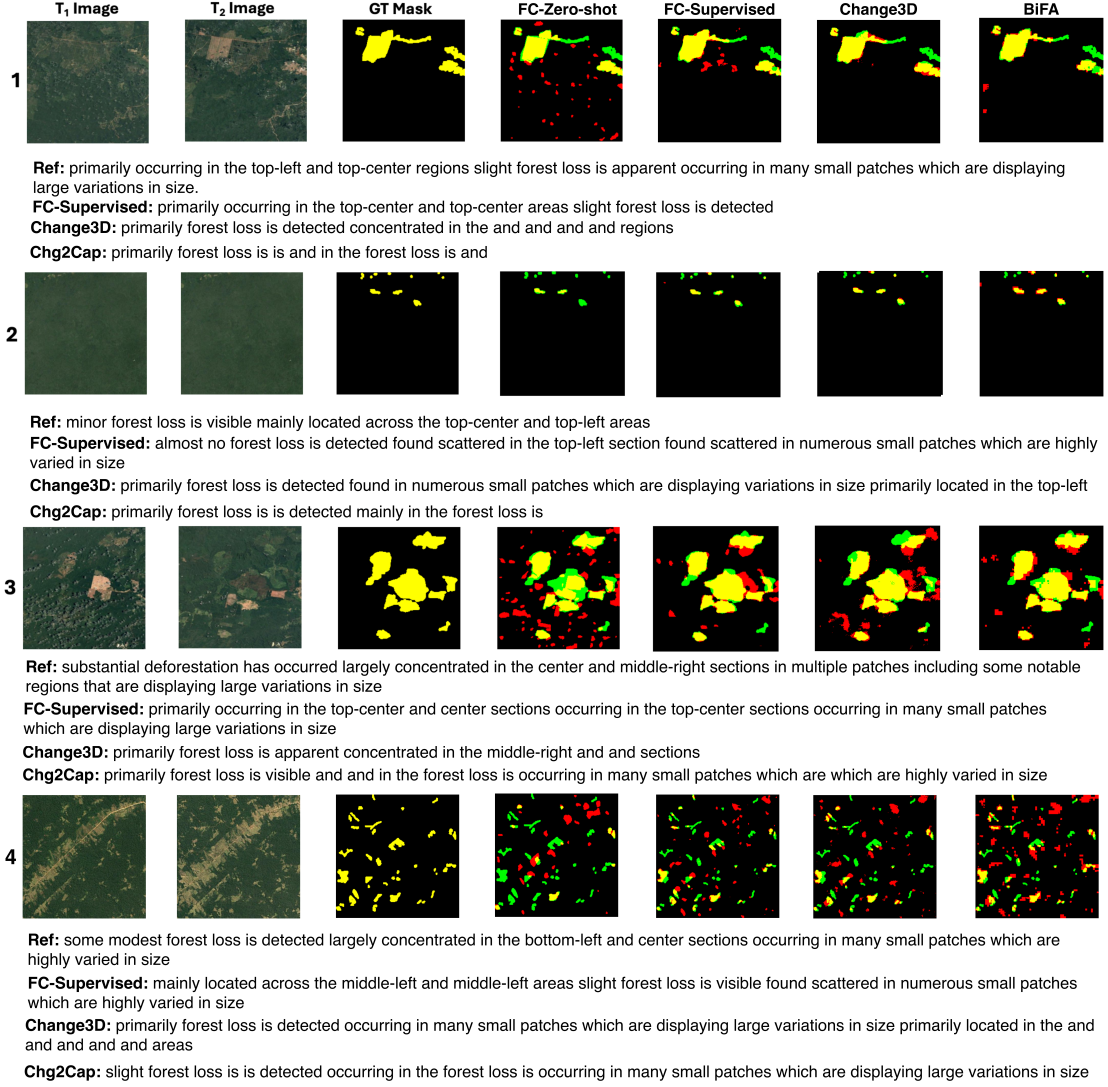


Figure 6: A selection of qualitative comparison results between the benchmarked models on the Forest-Change test set. Yellow indicates agreement with GT mask, red for false positives, green for false negatives.

high-quality annotations is therefore crucial, particularly to capture subtle, localised, and ecologically meaningful change processes. Integrating multiple modalities and various temporal sequence lengths would increase the variety of downstream tasks models could learn from the data.

Designing agentic VLM frameworks capable of providing further support for forest change analysis tasks is another important avenue. The current framework is limited to tasks auxiliary to change detection, captioning, and general reasoning. Enhanced visualisation tools and regression outputs can be applied for advanced ecological health assessments and biodiversity monitoring. If pursued through a single multi-task architecture, appropriate model structures and training strategies will need to be considered, with importance given to task balance and inter-task relationships. Although FC-Supervised contains architectural components that improve the ability to detect small and fine-grained change objects, performance on these subtle patterns remains limited. Future work should aim to de-

velop architectures that can reliably capture small-scale forest changes informed by ecological dynamics and domain-specific knowledge.

The reliance on few-shot examples within the system prompt also results in periodic task execution failures and is inefficient for scaling to more complex scenarios. In such cases, the LLM may misinterpret user instructions or fail to produce useful solutions. Expanding the agent’s toolset, integrating task-aware retrieval, and supporting a multi-agent framework, or Mixture-of-Experts system would markedly enhance robustness for a wide array of applications. Storing previous conversations in a knowledge base would further help to ground future LLM responses. Enabling zero-shot change captioning and embedding geographic knowledge could further ground reasoning and reduce the reliance on large labelled datasets.

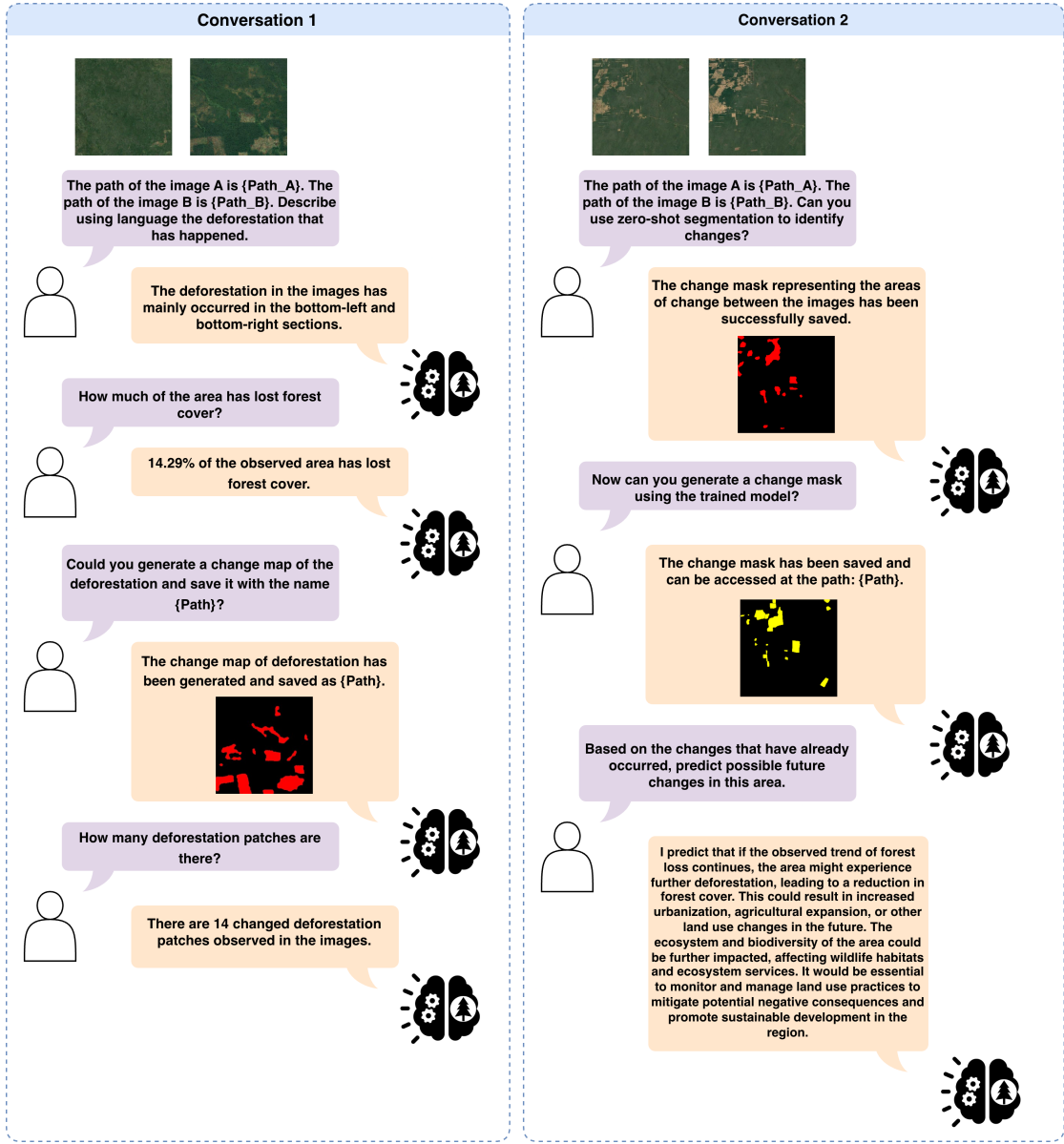


Figure 7: Conversation examples between users and Forest-Chat. Forest-Chat is capable of understanding users and orchestrating the relevant tools to answer questions relating to forest change detection, building upon the capabilities of Change-Agent.

7. Conclusion

Forest-Chat addresses the growing need for interpretable and accessible forest change analysis by integrating VLMs with a conversational interface. The system leverages the MCI model in combination with AnyChange to provide pixel-level change masks and semantic captions, enabling comprehensive understanding of bi-temporal forest imagery and forest loss events. The introduction of the Forest-Change dataset, which pairs change masks with descriptive captions, supports joint training for detection and captioning tasks, while multi-task learning balancing ensures effective optimisation across objectives. Supplementary tools, including a bi-temporal image captioning interface and a zero-shot point query interface, further facilitate interactive exploration and annotation, enhancing usability for researchers and practitioners.

Extensive experiments demonstrate that Forest-Chat can reliably detect and describe forest changes, with the underlying MCI model generalising well from an urban change context into a forest one, showing superior or competitive performance to SOTA models for both tasks. Incorporating an LLM with VLM capabilities lowers the barriers for engaging with RS data, highlighting the broader potential of interactive AI systems to improve interpretability, accessibility, and efficiency in environmental monitoring. This framework provides a foundation for future expansions, including scaling to larger and more diverse datasets, integrating domain-knowledge and additional modalities, and supporting richer natural language queries and tasks, advancing the development of intelligent tools for ecological research and forest monitoring.

CRediT authorship contribution statement

James Brock: Conceptualisation, Data curation, Formal analysis; Investigation, Methodology, Project administration, Software, Validation, Visualisation, Writing – original draft, Writing – review and editing. **Ce Zhang:** Supervision, Conceptualisation, Project administration, Writing – review and editing. **Nantheera Anantrasirichai:** Supervision, Writing – review and editing.

Declaration of competing interest

The authors declare that they have no known competing financial interests or personal relationships that could have appeared to influence the work reported in this paper.

Funding

This research did not receive any specific grant from funding agencies in the public, commercial, or not-for-profit sectors.

Acknowledgements

The authors wish to acknowledge and thank the financial support of the UK Research and Innovation (UKRI) [Grant ref EP/Y030796/1] and the University of Bristol. We would also like to thank colleagues and reviewers for their helpful feedback and discussions relating to this work.

Data availability

All data and code used in this work are available in the following GitHub repository: <https://github.com/JamesBrockUoB/ForestChat>.

Declaration of generative AI and AI-assisted technologies in the manuscript preparation process

During the preparation of this work the authors used ChatGPT and Claude to develop and debug experimental code, produce visualisation code, and format elements within the article, such as tables and equations. After using these tools, the authors reviewed and edited the content as needed and take full responsibility for the content of the published article.

References

Banerjee, S., Lavie, A., 2005. Meteor: An automatic metric for mt evaluation with improved correlation with human judgments, in: Proceedings of the acl workshop on intrinsic and extrinsic evaluation measures for machine translation and/or summarization, pp. 65–72.

Bazi, Y., Bashmal, L., Al Rahhal, M.M., Ricci, R., Melgani, F., 2024. Rs-llava: A large vision-language model for joint captioning and question answering in remote sensing imagery. *Remote Sensing* 16, 1477.

Cai, C., Xu, H., Chen, S., Yang, L., Weng, Y., Huang, S., Dong, C., Lou, X., 2023. Tree recognition and crown width extraction based on novel faster-rcnn in a dense loblolly pine environment. *Forests* 14, 863.

Cai, Z., Cao, M., Chen, H., Chen, K., Chen, K., et al., 2024. Internlm2 technical report. [arXiv:2403.17297](https://arxiv.org/abs/2403.17297).

Canion, H., 2021. Food and agriculture organization of the united nations—fao, in: The Europa directory of international organizations 2021. Routledge, pp. 297–305.

Chang, S., Ghamisi, P., 2023. Changes to captions: An attentional network for remote sensing change captioning. *IEEE Transactions on Image Processing* 32, 6047–6060.

Chen, H., Song, J., Han, C., Xia, J., Yokoya, N., 2024. Changemamba: Remote sensing change detection with spatiotemporal state space model. *IEEE Transactions on Geoscience and Remote Sensing* 62, 1–20.

Chen, Z., Badrinarayanan, V., Lee, C.Y., Rabinovich, A., 2018. Gradnorm: Gradient normalization for adaptive loss balancing in deep multitask networks, in: International conference on machine learning, PMLR. pp. 794–803.

Chen, Z., Ngiam, J., Huang, Y., Luong, T., Kretzschmar, H., Chai, Y., Anguelov, D., 2020. Just pick a sign: Optimizing deep multitask models with gradient sign dropout. *Advances in Neural Information Processing Systems* 33, 2039–2050.

Crawshaw, M., 2020. Multi-task learning with deep neural networks: A survey. *arXiv preprint arXiv:2009.09796*.

Debus, A., Beauchamp, E., Acworth, J., Ewolo, A., Kamga, J., Verhegghen, A., Zébazé, C., Lines, E.R., 2024. A labelled dataset to classify direct deforestation drivers from earth observation imagery in cameroon. *Scientific Data* 11, 564.

Deng, P., Zhou, W., Wu, H., 2025. Changechat: An interactive model for remote sensing change analysis via multi-modal instruction tuning, in: ICASSP 2025-2025 IEEE International Conference on Acoustics, Speech and Signal Processing (ICASSP), IEEE. pp. 1–5.

Du, S., Tang, S., Wang, W., Li, X., Guo, R., 2023. Tree-gpt: Modular large language model expert system for forest remote sensing image understanding and interactive analysis. *The International Archives of the Photogrammetry, Remote Sensing and Spatial Information Sciences* 48, 1729–1736.

Gao, P., Yamasaki, T., Imoto, K., 2024. Ve-kd: Vocabulary-expansion knowledge-distillation for training smaller domain-specific language models, in: Findings of the Association for Computational Linguistics: EMNLP 2024, pp. 15046–15059.

Ge, Y., Hua, W., Mei, K., Tan, J., Xu, S., Li, Z., Zhang, Y., et al., 2023. Openagi: When llm meets domain experts. *Advances in Neural Information Processing Systems* 36, 5539–5568.

Gorelick, N., Hancher, M., Dixon, M., Ilyushchenko, S., Thau, D., Moore, R., 2017. Google earth engine: Planetary-scale geospatial analysis for everyone. *Remote sensing of Environment* 202, 18–27.

Green, T., Alam, S., McIntosh-Smith, S., Gilham, R., Wishart, W., 2025. Evaluation of the nvidia grace superchip in the hpe/cray xd isambard 3 supercomputer. *CUG 2025* 2025, 93.

Gu, A., Dao, T., 2024. Mamba: Linear-time sequence modeling with selective state spaces. URL: <https://arxiv.org/abs/2312.00752>, arXiv:2312.00752.

Guo, H., Su, X., Wu, C., Du, B., Zhang, L., Li, D., 2024. Remote sensing chatgpt: Solving remote sensing tasks with chatgpt and visual models, in: *IGARSS 2024-2024 IEEE International Geoscience and Remote Sensing Symposium*, IEEE. pp. 11474–11478.

Guo, Z., Wang, T.J., Laaksonen, J., 2022. Clip4idc: Clip for image difference captioning, in: *Proceedings of the 2nd Conference of the Asia-Pacific Chapter of the Association for Computational Linguistics and the 12th International Joint Conference on Natural Language Processing (Volume 2: Short Papers)*, pp. 33–42.

Hansen, M.C., Potapov, P.V., Moore, R., Hancher, M., Turubanova, S.A., Tyukavina, A., Thau, D., Stehman, S.V., Goetz, S.J., Loveland, T.R., et al., 2013. High-resolution global maps of 21st-century forest cover change. *science* 342, 850–853.

Hartanti, B.S.I., Vito, V., Arymurthy, A.M., Alfa Krisnadhi, A., Setiyoko, A., 2023. Multimodal supercon: classifier for drivers of deforestation in indonesia. *Journal of Applied Remote Sensing* 17, 036502–036502.

Hewarathna, A.I., Hamlin, L., Charles, J., Vigneshwaran, P., George, R., Thusethan, S., Wimalasooriya, C., Shanmugam, B., 2024. Change detection for forest ecosystems using remote sensing images with siamese attention u-net. *Technologies* 12, 160.

Hu, Y., Yuan, J., Wen, C., Lu, X., Liu, Y., Li, X., 2025. Rsgpt: A remote sensing vision language model and benchmark. *IS-PRS Journal of Photogrammetry and Remote Sensing* 224, 272–286.

Irvin, J.A., Liu, E.R., Chen, J.C., Dormoy, I., Kim, J., Khanna, S., Zheng, Z., Ermon, S., 2025. TEOChat: A large vision-language assistant for temporal earth observation data, in: *The Thirteenth International Conference on Learning Representations*. URL: <https://openreview.net/forum?id=pZz0n0roGv>.

Isaienkov, K., Yushchuk, M., Khramtsov, V., Seliverstov, O., 2020. Deep learning for regular change detection in ukrainian forest ecosystem with sentinel-2. *IEEE Journal of Selected Topics in Applied Earth Observations and Remote Sensing* 14, 364–376.

Kendall, A., Gal, Y., Cipolla, R., 2018. Multi-task learning using uncertainty to weigh losses for scene geometry and semantics, in: *Proceedings of the IEEE conference on computer vision and pattern recognition*, pp. 7482–7491.

Kirillov, A., Mintun, E., Ravi, N., Mao, H., Rolland, C., Gustafson, L., Xiao, T., Whitehead, S., Berg, A.C., Lo, W.Y., et al., 2023. Segment anything, in: *Proceedings of the IEEE/CVF international conference on computer vision*, pp. 4015–4026.

Kuckreja, K., Danish, M.S., Naseer, M., Das, A., Khan, S., Khan, F.S., 2024. Geochat: Grounded large vision-language model for remote sensing, in: *Proceedings of the IEEE/CVF Conference on Computer Vision and Pattern Recognition*, pp. 27831–27840.

Lee, M.G., Cho, H.B., Youm, S.K., Kim, S.W., 2023. Detection of pine wilt disease using time series uav imagery and deep learning semantic segmentation. *Forests* 14, 1576.

Li, C., Xiao, M., Liu, Y., 2024a. Prospects for ai applications in forest protection: Technologies, challenges, and future developments. *Advances in Resources Research* 4, 362–380.

Li, J., Cai, Y., Li, Q., Kou, M., Zhang, T., 2024b. A review of remote sensing image segmentation by deep learning methods. *International Journal of Digital Earth* 17, 2328827.

Li, X., Sun, B., Wu, Z., Li, S., Guo, H., 2025. Cd4c: Change detection for remote sensing image change captioning. *IEEE Journal of Selected Topics in Applied Earth Observations and Remote Sensing* .

Li, X., Wen, C., Hu, Y., Yuan, Z., Zhu, X.X., 2024c. Vision-language models in remote sensing: Current progress and future trends. *IEEE Geoscience and Remote Sensing Magazine* 12, 32–66.

Li, Y., Xu, W., Li, G., Yu, Z., Wei, Z., Wang, J., Peng, M., 2024d. Unirs: Unifying multi-temporal remote sensing tasks through vision language models. *arXiv preprint arXiv:2412.20742* .

Lin, C.Y., 2004. Rouge: A package for automatic evaluation of summaries, in: *Text summarization branches out*, pp. 74–81.

Lin, F.C., Shiu, Y.S., Wang, P.J., Wang, U.H., Lai, J.S., Chuang, Y.C., 2024. A model for forest type identification and forest regeneration monitoring based on deep learning and hyperspectral imagery. *Ecological Informatics* 80, 102507.

Lines, E.R., Allen, M., Cabo, C., Calders, K., Debus, A., Grieve, S.W., Miltiadou, M., Noach, A., Owen, H.J., Puliti, S., 2022. Ai applications in forest monitoring need remote

sensing benchmark datasets, in: 2022 IEEE international conference on big data (big data), IEEE. pp. 4528–4533.

Liu, B., Liu, X., Jin, X., Stone, P., Liu, Q., 2021. Conflict-averse gradient descent for multi-task learning. *Advances in Neural Information Processing Systems* 34, 18878–18890.

Liu, C., Chen, K., Zhang, H., Qi, Z., Zou, Z., Shi, Z., 2024. Change-agent: Towards interactive comprehensive remote sensing change interpretation and analysis. *IEEE Transactions on Geoscience and Remote Sensing* .

Liu, C., Zhang, J., Chen, K., Wang, M., Zou, Z., Shi, Z., 2025. Remote sensing spatiotemporal vision–language models: A comprehensive survey. *IEEE Geoscience and Remote Sensing Magazine* .

Liu, C., Zhao, R., Chen, H., Zou, Z., Shi, Z., 2022. Remote sensing image change captioning with dual-branch transformers: A new method and a large scale dataset. *IEEE Transactions on Geoscience and Remote Sensing* 60, 1–20.

Liu, X., Lian, Z., 2024. Rsunivlm: A unified vision language model for remote sensing via granularity-oriented mixture of experts. *arXiv preprint arXiv:2412.05679* .

Lu, S., Guo, J., Zimmer-Dauphinee, J.R., Nieuwsma, J.M., Wang, X., Wernke, S.A., Huo, Y., et al., 2025. Vision foundation models in remote sensing: A survey. *IEEE Geoscience and Remote Sensing Magazine* .

Mu, Y., Xiong, Z., Wang, Y., Shahzad, M., Essl, F., Kreft, H., van Kleunen, M., Zhu, X.X., 2025. Globalgeotree: A multi-granular vision-language dataset for global tree species classification. *Earth System Science Data Discussions* 2025, 1–34.

Nguyen, T.A., Rußwurm, M., Lenczner, G., Tuia, D., 2024. Multi-temporal forest monitoring in the swiss alps with knowledge-guided deep learning. *Remote Sensing of Environment* 305, 114109.

openai, Applin, S., Adesso, G., Ashfaq, R., Bai, M., Brammer, M., Fecht, E., Goodman, A., Grossman, S., Groh, M., Kirk, H.R., Gunitsky, S., Huang, Y., Kahn, L., Kumar, S., Madrid-Morales, D., Motoki, F., Ovadya, A., Peters, U., Robinson, M., Röttger, P., Wasserman, H., Wehsener, A., Walker, L., Vidgen, B., Zhu, J., 2023. Gpt-4v(ision) system card URL: https://opal.latrobe.edu.au/articles/report/GPT-4V_ision_System_Card/25479208, doi:10.26181/25479208.v1.

Ouaknine, A., Kattenborn, T., Laliberté, E., Rolnick, D., 2025. Openforest: a data catalog for machine learning in forest monitoring. *Environmental Data Science* 4, e15.

Papineni, K., Roukos, S., Ward, T., Zhu, W.J., 2002. Bleu: a method for automatic evaluation of machine translation, in: Proceedings of the 40th annual meeting of the Association for Computational Linguistics, pp. 311–318.

Peng, D., Liu, X., Zhang, Y., Guan, H., Li, Y., Bruzzone, L., 2025. Deep learning change detection techniques for optical remote sensing imagery: Status, perspectives and challenges. *International Journal of Applied Earth Observation and Geoinformation* 136, 104282.

Radford, A., Kim, J.W., Hallacy, C., Ramesh, A., Goh, G., Agarwal, S., Sastry, G., Askell, A., Mishkin, P., Clark, J., et al., 2021. Learning transferable visual models from natural language supervision, in: International conference on machine learning, PMLR. pp. 8748–8763.

Schick, T., Dwivedi-Yu, J., Dessì, R., Raileanu, R., Lomeli, M., Hambro, E., Zettlemoyer, L., Cancedda, N., Scialom, T., 2023. Toolformer: Language models can teach themselves to use tools. *Advances in Neural Information Processing Systems* 36, 68539–68551.

Sener, O., Koltun, V., 2018. Multi-task learning as multi-objective optimization. *Advances in neural information processing systems* 31.

Shi, J., Zhang, M., Hou, Y., Zhi, R., Liu, J., 2024. A multi-task network and two large scale datasets for change detection and captioning in remote sensing images. *IEEE Transactions on Geoscience and Remote Sensing* .

Tao, L., Zhang, H., Jing, H., Liu, Y., Yan, D., Wei, G., Xue, X., 2025. Advancements in vision–language models for remote sensing: Datasets, capabilities, and enhancement techniques. *Remote Sensing* 17, 162.

Taylor, R., Dudley, N., Stolton, S., Shapiro, A., 2015. Deforestation fronts: 11 places where most forest loss is projected between 2010 and 2030, in: Proceedings of the XIV World Forestry Congress, Durban, South Africa, pp. 7–11.

Touvron, H., Lavril, T., Izacard, G., Martinet, X., Lachaux, M.A., Lacroix, T., Rozière, B., Goyal, N., Hambro, E., Azhar, F., et al., 2023. Llama: Open and efficient foundation language models. *arXiv preprint arXiv:2302.13971* .

Vaswani, A., Shazeer, N., Parmar, N., Uszkoreit, J., Jones, L., Gomez, A.N., Kaiser, Ł., Polosukhin, I., 2017. Attention is all you need. *Advances in neural information processing systems* 30.

Vedantam, R., Lawrence Zitnick, C., Parikh, D., 2015. Cider: Consensus-based image description evaluation, in: Proceedings of the IEEE conference on computer vision and pattern recognition, pp. 4566–4575.

Wang, J., Chen, T., Zheng, L., Tie, J., Zhang, Y., Chen, P., Luo, Z., Song, Q., 2025. A multi-scale remote sensing semantic segmentation model with boundary enhancement based on unetformer. *Scientific Reports* 15, 1–19.

Wang, Y., Yu, W., Kopp, M., Ghamisi, P., 2024. Changeminds: Multi-task framework for detecting and describing changes in remote sensing. *arXiv preprint arXiv:2410.10047* .

Watch, G.F., 2014. Global forest watch. <http://www.globalforestwatch.org>. World Resources Institute. Accessed: 2025-08-10.

Wegler, M., Kuenzer, C., 2024. Potential of earth observation to assess the impact of climate change and extreme weather events in temperate forests—a review. *Remote Sensing* 16, 2224.

Xie, E., Wang, W., Yu, Z., Anandkumar, A., Alvarez, J.M., Luo, P., 2021. Segformer: Simple and efficient design for semantic segmentation with transformers. *Advances in neural information processing systems* 34, 12077–12090.

Xu, W., Yu, Z., Mu, B., Wei, Z., Zhang, Y., Li, G., Peng, M., 2024. Rs-agent: Automating remote sensing tasks through intelligent agent. *arXiv preprint arXiv:2406.07089* .

Yang, C., Li, Z., Jiao, H., Gao, Z., Zhang, L., 2025a. Enhancing perception of key changes in remote sensing image change captioning. *IEEE Transactions on Image Processing* .

Yang, M., Chen, L., Zhou, J., 2025b. Change-up: Advancing visualization and inference capability for multi-level remote sensing change interpretation, in: *Proceedings of the 33rd ACM International Conference on Multimedia*, pp. 15–24.

Yao, S., Zhao, J., Yu, D., Du, N., Shafran, I., Narasimhan, K., Cao, Y., 2023. React: Synergizing reasoning and acting in language models, in: *The eleventh international conference on learning representations*. Publisher Copyright: © 2023 11th International Conference on Learning Representations, ICLR 2023. All rights reserved.; 11th International Conference on Learning Representations, ICLR 2023 ; Conference date: 01-05-2023 Through 05-05-2023.

Yu, T., Kumar, S., Gupta, A., Levine, S., Hausman, K., Finn, C., 2020. Gradient surgery for multi-task learning. *Advances in neural information processing systems* 33, 5824–5836.

Yu, Y., Zhuang, Y., Zhang, J., Meng, Y., Ratner, A.J., Krishna, R., Shen, J., Zhang, C., 2023. Large language model as attributed training data generator: A tale of diversity and bias. *Advances in neural information processing systems* 36, 55734–55784.

Yun, T., Li, J., Ma, L., Zhou, J., Wang, R., Eichhorn, M.P., Zhang, H., 2024. Status, advancements and prospects of deep learning methods applied in forest studies. *International Journal of Applied Earth Observation and Geoinformation* 131, 103938.

Zeng, Z., Xie, Y., Zhang, H., Chen, C., Chen, B., Wang, Z., 2024. Meacap: Memory-augmented zero-shot image captioning, in: *Proceedings of the IEEE/CVF conference on computer vision and pattern recognition*, pp. 14100–14110.

Zhang, C., Wang, S., 2024. Good at captioning bad at counting: Benchmarking gpt-4v on earth observation data, in: *Proceedings of the IEEE/CVF Conference on Computer Vision and Pattern Recognition*, pp. 7839–7849.

Zhang, H., Chen, H., Zhou, C., Chen, K., Liu, C., Zou, Z., Shi, Z., 2024a. Bifa: Remote sensing image change detection with bitemporal feature alignment. *IEEE Transactions on Geoscience and Remote Sensing* 62, 1–17.

Zhang, H., Chen, K., Liu, C., Chen, H., Zou, Z., Shi, Z., 2025a. Cdmamba: Incorporating local clues into mamba for remote sensing image binary change detection. *IEEE Transactions on Geoscience and Remote Sensing* .

Zhang, W., Cai, M., Zhang, T., Zhuang, Y., Mao, X., 2024b. Earthgpt: A universal multimodal large language model for multisensor image comprehension in remote sensing domain. *IEEE Transactions on Geoscience and Remote Sensing* 62, 1–20.

Zhang, Y., Yang, Q., 2021. A survey on multi-task learning. *IEEE transactions on knowledge and data engineering* 34, 5586–5609.

Zhang, Z., Shen, H., Zhao, T., Chen, B., Guan, Z., Wang, Y., Jia, X., Cai, Y., Shang, Y., Yin, J., 2025b. Georsmllm: A multimodal large language model for vision-language tasks in geoscience and remote sensing. *arXiv preprint arXiv:2503.12490* .

Zheng, Z., Zhong, Y., Zhang, L., Ermon, S., 2024. Segment any change. *Advances in Neural Information Processing Systems* 37, 81204–81224.

Zhu, D., Huang, X., Huang, H., Zhou, H., Shao, Z., 2025. Change3d: Revisiting change detection and captioning from a video modeling perspective, in: *Proceedings of the Computer Vision and Pattern Recognition Conference*, pp. 24011–24022.

Zhu, Y., Li, L., Chen, K., Liu, C., Zhou, F., Shi, Z., 2024. Semantic-cc: Boosting remote sensing image change captioning via foundational knowledge and semantic guidance. *IEEE Transactions on Geoscience and Remote Sensing* .

Zou, S., Wei, Y., Xie, Y., Lao, M., Luan, X., 2025. Remote sensing image change captioning: A comprehensive review: S. zou et al. *International Journal of Multimedia Information Retrieval* 14, 26.

Appendix A. Supplementary Results

Table A.1: **Full MTL strategy change detection and change captioning ablation results.** Mean \pm standard deviation across configurations, with three runs each. Bold indicates the best mean value per metric within each group when the improvement is clearly distinguishable relative to standard deviation.

MTL Configuration	MIoU	IoU_{nc}	IoU_c	B1	B2	B3	B4	METEOR	$ROUGE_L$	CIDEr-D
Equal	67.10 \pm 0.07	96.12 \pm 0.09	38.07 \pm 0.09	67.88\pm4.55	56.35\pm4.88	47.55 \pm 5.31	40.17 \pm 5.84	28.22 \pm 2.61	48.52 \pm 3.46	38.79\pm10.90
+ CAGrad	67.02 \pm 0.30	96.29 \pm 0.15	37.75 \pm 0.45	65.09 \pm 3.51	55.49 \pm 3.41	47.87\pm4.04	41.55\pm4.46	28.28 \pm 1.17	49.39 \pm 1.20	38.49 \pm 5.62
+ PCGrad	67.46 \pm 0.38	96.18 \pm 0.11	38.74 \pm 0.90	64.28 \pm 3.26	52.92 \pm 3.29	44.22 \pm 3.44	37.56 \pm 1.96	27.46 \pm 1.25	46.72 \pm 1.43	34.72 \pm 6.66
+ GradDrop	67.77\pm0.46	96.21 \pm 0.10	39.33\pm0.81	61.12 \pm 3.83	50.77 \pm 4.25	41.67 \pm 4.32	34.44 \pm 3.56	26.25 \pm 2.20	45.56 \pm 2.78	30.29 \pm 8.85
EDWA	67.30 \pm 0.49	96.20 \pm 0.25	38.40 \pm 0.92	66.16 \pm 4.91	55.54 \pm 5.12	46.42 \pm 4.14	39.79 \pm 3.68	28.40 \pm 3.54	49.02 \pm 3.48	36.16 \pm 7.21
+ CAGrad	66.98 \pm 0.73	96.16 \pm 0.22	37.79 \pm 1.27	63.30 \pm 1.91	52.17 \pm 3.57	43.12 \pm 4.28	35.85 \pm 4.83	26.73 \pm 0.40	46.59 \pm 1.52	29.96 \pm 4.05
+ PCGrad	66.32 \pm 0.68	96.13 \pm 0.12	36.52 \pm 1.51	65.84 \pm 3.61	55.36 \pm 2.87	46.55 \pm 2.63	39.64 \pm 2.84	27.53 \pm 2.13	47.54 \pm 2.11	35.70 \pm 4.88
+ GradDrop	66.90 \pm 0.63	96.26 \pm 0.19	37.54 \pm 1.55	62.52 \pm 6.11	51.68 \pm 5.90	42.71 \pm 5.17	35.63 \pm 5.51	27.21 \pm 4.19	47.69 \pm 4.98	30.69 \pm 6.13
Uncertainty	67.30 \pm 0.23	96.41\pm0.20	38.19 \pm 0.44	64.29 \pm 2.76	54.64 \pm 2.45	46.66 \pm 2.42	40.19 \pm 2.64	28.41 \pm 2.06	48.67 \pm 2.66	35.58 \pm 11.46
+ CAGrad	67.49 \pm 0.49	96.35 \pm 0.06	38.64 \pm 0.92	62.64 \pm 1.99	52.83 \pm 1.24	45.43 \pm 0.27	39.61 \pm 0.62	28.31 \pm 1.45	49.22 \pm 2.11	36.71 \pm 5.89
+ PCGrad	66.82 \pm 0.48	96.26 \pm 0.17	37.37 \pm 0.81	63.04 \pm 4.75	52.89 \pm 5.14	44.07 \pm 5.74	37.20 \pm 6.42	26.77 \pm 3.24	47.18 \pm 4.32	34.68 \pm 2.66
+ GradDrop	66.48 \pm 0.38	95.86 \pm 0.43	37.11 \pm 0.55	65.57 \pm 4.09	55.18 \pm 4.93	46.42 \pm 5.05	39.39 \pm 5.27	28.29 \pm 2.29	49.61\pm3.08	27.97 \pm 5.81

Table A.2: **Full MTL change detection and captioning ablation results shown as percentage changes relative to baseline.** Only $\Delta\%$ values are reported; positive/negative values indicate improvement or decline compared to the baseline configuration respectively. Bold indicates the largest improvement among non-baseline configurations per metric when the improvement is clearly distinguishable.

MTL Configuration	MIoU	IoU_{nc}	IoU_c	B1	B2	B3	B4	METEOR	$ROUGE_L$	CIDEr-D
Baseline (Equal)	–	–	–	–	–	–	–	–	–	–
+ CAGrad	-0.12	+0.18	-0.84	-4.11	-1.53	+0.67	+3.44	+0.21	+1.79	-0.77
+ PCGrad	+0.54	+0.06	+1.76	-5.30	-6.09	-7.00	-6.50	-2.69	-3.71	-10.49
+ GradDrop	+1.00	+0.09	+3.31	-9.96	-9.90	-12.37	-14.26	-6.98	-6.10	-21.91
EDWA	+0.30	+0.08	+0.87	-2.53	-1.44	-2.38	-0.95	+0.64	+1.03	-6.78
+ CAGrad	-0.18	+0.04	-0.74	-6.75	-7.42	-9.32	-10.75	-5.28	-3.98	-22.76
+ PCGrad	-1.16	+0.01	-4.07	-3.01	-1.76	-2.10	-1.32	-2.45	-2.02	-7.97
+ GradDrop	-0.30	+0.15	-1.39	-7.90	-8.29	-10.18	-11.30	-3.58	-1.71	-20.88
Uncertainty	+0.30	+0.30	+0.32	-5.29	-3.03	-1.87	+0.05	+0.67	+0.31	-8.28
+ CAGrad	+0.58	+0.24	+1.50	-7.72	-6.25	-4.46	-1.39	+0.32	+1.44	-5.36
+ PCGrad	-0.42	+0.15	-1.84	-7.13	-6.14	-7.32	-7.39	-5.14	-2.76	-10.60
+ GradDrop	-0.92	-0.27	-2.52	-3.40	-2.08	-2.38	-1.94	+0.25	+2.25	-27.89

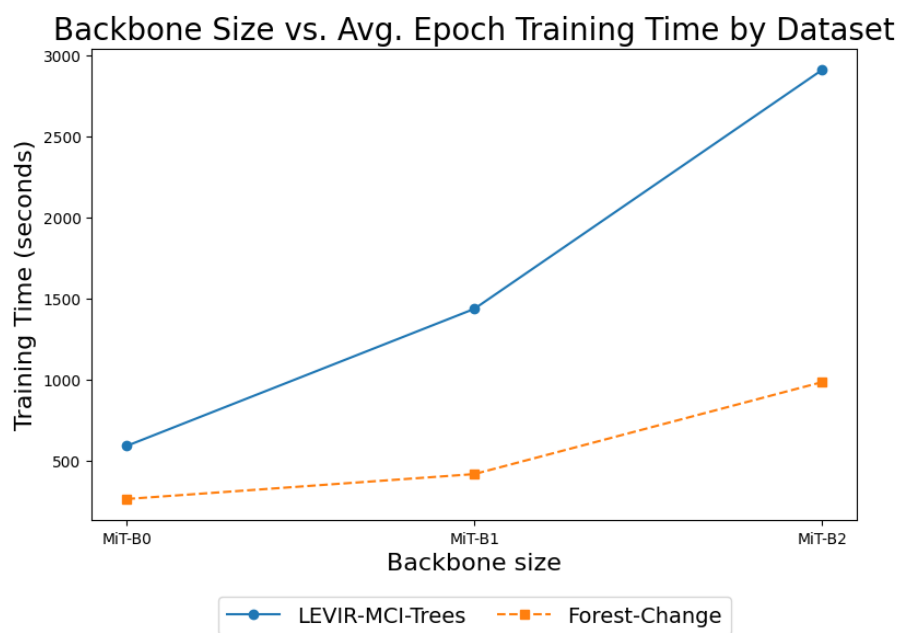


Figure A.1: Training Time Comparison by Backbone Size for Each Dataset. The lines show the training time for one epoch (mean over three runs) per backbone size for the LEVIR-MCI-Trees and Forest-Change datasets.